

Stereochemistry and Spin State in Four-Coordinate Transition Metal Compounds

Jordi Cirera, Eliseo Ruiz, and Santiago Alvarez*

Departament de Química Inorgànica and Institut de Química Teòrica i Computacional,
Universitat de Barcelona, Diagonal 647, 08028 Barcelona, Spain

Received November 20, 2007

A systematic DFT computational study of the stereochemistry associated with each spin state for first transition series four-coordinate d^n ($n = 0-10$) homoleptic metal complexes is presented. The stereochemistry of $[\text{MMe}_4]^{x-}$ complexes in the 21 spin configurations analyzed can be predicted from the d orbital occupation in the ideal tetrahedral geometry, grouped in three families with tetrahedral, square planar, or intermediate structures that can be described in some cases as sawhorses. The effect of the following factors on the spin state and stereochemical preferences has also been studied: (a) substitution of the σ -donor methyl ligands by π -donor chlorides, (b) a high (+ 4) oxidation state of the metal, and (c) substitution of the metal atom by a second transition series one. Through those factors, low-spin tetrahedral structures can be achieved, as summarized by a magic cube.

Introduction

Four-coordinate complexes constitute one of the commonest building blocks in transition metal chemistry, second only to their six-coordinate relatives. Despite their ubiquity throughout the periodic table, only a few general rules are established for the stereochemical and spin-state preferences of four-coordinate complexes. Certainly, it is well established that oxoanions of metal atoms in high-oxidation states are tetrahedral, that the same geometry is found among tetrahalo complexes, and that d^8 metal ions, such as Rh^I , Ir^I , Pd^{II} , Pt^{II} , and Au^{III} are almost invariably square planar.¹ Recently,² we analyzed the structures of more than 13 000 four-coordinate transition metal centers from the point of view of their tetrahedral and square planar shape measures and extended the previously established empirical trends as follows: (i) d^0 , d^1 , d^2 , d^5 , and d^{10} configurations prefer the tetrahedral geometry; (ii) d^8 and d^9 complexes show a strong preference for the square planar geometry; (iii) d^3 , d^4 , d^6 , and d^7 metals appear in either tetrahedral or square planar structures; (iv) a significant fraction of d^9 ions have structures intermediate between square planar and tetrahedral; and (v)

a large number of structures that cannot be adequately described as tetrahedral, square planar, or intermediate are found for d^3 , d^6 , and d^{10} complexes.

However, as pointed out by Poli,³ it is clear that the stereochemical preference of a given metal ion depends on its spin state. We therefore started a project that aimed at establishing the theoretical rules that may determine the choice of geometry and spin state in tetracoordinate complexes, confronting them with the available experimental information (both structural and magnetic), confirming and completing, if possible, the empirical rules established previously. Such rules should ultimately allow us to predict both the stereochemistry and the spin state of a given combination of metal ion and ligands. In this paper, we present the results of calculations based on density functional theory for a variety of four-coordinate model complexes, in which we systematically analyze the effect on the stereochemistry of (a) the number of d electrons, (b) the spin state, (c) the metal oxidation state, (d) the σ donor or π donor nature of the ligands, and (e) the position of the metal within a group of the periodic table. Stereochemical constraints imposed by bi- and multidentate ligands that were discussed in our previous structural study² have been disregarded for the present study, and only monodentate ligands will be considered.

* To whom correspondence should be addressed. E-mail: santiago.alvarez@qi.ub.es. Fax: 34 93-490-7225.

(1) Atkins, P.; Overton, T.; Rourke, J.; Weller, M.; Armstrong, F. *Shriver & Atkins Inorganic Chemistry*; Oxford University Press: Oxford, U.K., 2006.

(2) Cirera, J.; Alemany, P.; Alvarez, S. *Chem.—Eur. J.* **2004**, *10*, 190.

(3) (a) Poli, R. *Chem. Rev.* **1996**, *96*, 2135. (b) Poli, R. *J. Organomet. Chem.* **2004**, *689*, 4291.

Conceptual Framework for this Study

Before presenting the results of our study, it is convenient to establish the concepts and nomenclature that will be used to make the discussion as simple and precise as possible. Since we will worry about the combination of spin state and stereochemistry that characterize each particular compound, let us first establish the conventions for naming both the stereochemistry and the spin state of the molecules studied. On the one hand, we consider three ideal four-vertex geometries: the tetrahedron, the square, and the sawhorse or seesaw. These geometries will be represented throughout this paper by their polyhedral symbols,⁴ *T4*, *SP4*, and *SS4*, respectively. Because we are dealing only with four-coordinate complexes, the numerical suffix is superfluous, and we will in most cases omit it and use *T*, *SP*, and *SS* as stereochemical descriptors. For the present discussion, in which we will be referring once and again to a given combination of stereochemistry and spin state, it is important to name such combinations with a single word, as explained in the next paragraphs.

Let us recall first that when two chemical compounds have the same composition and atomic connectivity but different spatial arrangement of their atoms, they are called *stereoisomers*. In the domain of transition metal compounds, we can mention as an example the $[\text{CuBr}_4]^{2-}$ anion, which presents varying geometries between the square and the tetrahedron, even in the same crystal structure.⁵ We notice that in this case the spin state is always the same, $S = 1/2$. To cite just another example, let us recall also pentacoordinate complexes, such as $[\text{Mn}(\text{CO})_5]^-$, that can be found in either a square pyramidal⁶ or trigonal bipyramidal⁷ stereochemistry, both with the same spin state.

The spin-crossover complexes,⁸ such as $[\text{Fe}(\text{phen})_2(\text{NCS})_2]$, present a different type of isomerism. In its low-temperature form (130 K), this compound is diamagnetic ($S = 0$), whereas its high-temperature form is paramagnetic (e.g., $S = 2$ at 293 K), has a different visible spectrum⁹ (i.e., different color) and significantly longer Fe–N bond distances. Therefore, the low- and high-temperature forms should indeed be considered different chemical compounds with clearly different chemical and physical properties, even if both have the same stereochemistry, with an octahedral coordination sphere around the Fe atom.¹⁰ These two forms are thus spin isomers, or *spinomers*, because they differ in their spin state but not in stereochemistry.

Finally, there may be cases in which two isomers differ in both stereochemistry and spin state that should be referred

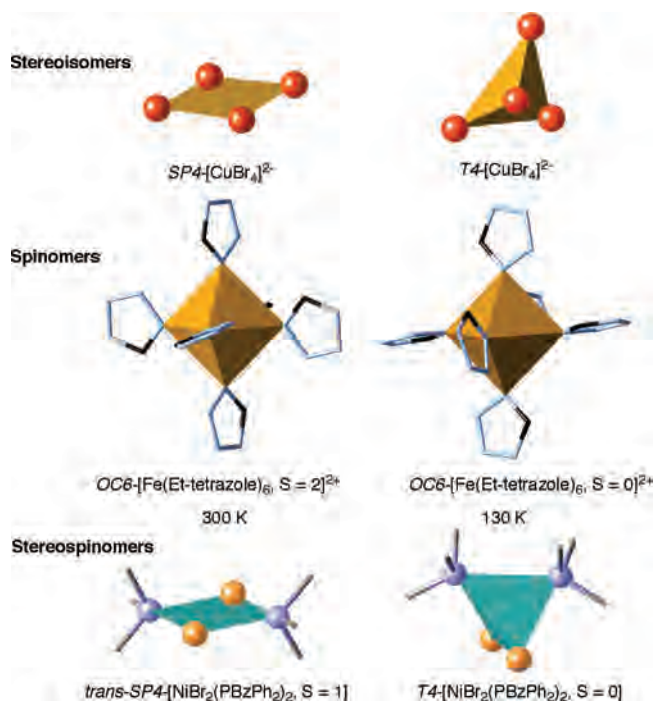


Figure 1. Examples of isomerism types that involve coordination geometry, spin state, or both: stereoisomeric anions in (picolyniumammonim)[CuBr_4],⁵ spinomeric cations in $[\text{Fe}(\text{Et-tetrazole})_6](\text{PF}_6)_2$ ¹³ and stereospinomerism in $[\text{Ni}(\text{PBzPh})_2\text{Br}_2]$.¹¹ The polyatomic ligands have been trimmed for clarity.

to as *stereospinomers*. As an example, consider the $[\text{Ni}(\text{PR}_3)_2\text{X}_2]$ complexes that exist in either square planar or tetrahedral geometries and which may even coexist in equilibrium. This is the case of $[\text{Ni}(\text{PBzPh})_2\text{Br}_2]$, which presents in the same crystal structure¹¹ one tetrahedral molecule with a triplet spin state and a square planar molecule with a spinless ground state.

For unambiguous reference to spinomers or stereospinomers, we propose to include in the formula of such complexes explicit reference to the spin state when it is known (Figure 1). Although there is a tendency to use the terms *high-spin* and *low-spin* to distinguish such cases, we have recently shown that such a labeling is arbitrary in some cases and may be confusing.¹² Inclusion of the spin state in the formula can be omitted when there is no ambiguity, as in the case of Cu^{II} compounds, much in the same way that stereochemical descriptors are often omitted. In Figure 1, we provide one example of each of the types of isomerism discussed here to illustrate the use of formulas with stereochemical and spin-state indications.

We must stress that the definition of spinomers given here is different from the concept of *bond stretch isomerism*.¹⁴ Two compounds are said to be bond-stretch isomers if they

- Connelly, N. G.; Damhus, T.; Hartshorn, R. M.; Hutton, A. T. *Nomenclature of Inorganic Chemistry. IUPAC Recommendations 2005*; RSC Publishing: Cambridge, U.K., 2005.
- Long, G. S.; Wei, M.; Willet, R. D. *Inorg. Chem.* **1997**, *36*, 3102.
- Seidel, R.; Schnautz, B.; Henkel, G. *Angew. Chem., Int. Ed.* **1996**, *35*, 1710.
- Hillier, A. C.; Sella, A.; Elsegood, M. R. J. *J. Organomet. Chem.* **2002**, *664*, 298.
- Real, J. A.; Gaspar, A. B.; Muñoz, M. C. *Dalton Trans.* **2005**, 2062.
- König, E.; Madeja, K. *Inorg. Chem.* **1967**, *6*, 48.
- Note, however, that for trischelate complexes there are small conformational differences between the low- and high-spin forms that imply different degrees of Bailar distortions of the octahedron. See: Alvarez, S. *J. Am. Chem. Soc.* **2003**, *125*, 6795.

- Kilbourn, B. T.; Powell, H. M. *J. Chem. Soc. A* **1970**, 1688.
- Alvarez, S.; Cirera, J. *Angew. Chem., Int. Ed.* **2006**, *45*, 3012.
- Jeftić, J.; Hinek, R.; Capelli, S. C.; Hauser, A. *Inorg. Chem.* **1997**, *36*, 3080.
- (a) Stohrer, W. D.; Hoffmann, R. *J. Am. Chem. Soc.* **1972**, *94*, 779. (b) Jean, Y.; Lledós, A.; Burdett, J. K.; Hoffmann, R. *J. Am. Chem. Soc.* **1988**, *110*; (c) Jean, Y.; Lledós, A.; Burdett, J. K.; Hoffmann, R. *J. Chem. Soc., Chem. Commun.* **1988**, 140. (d) Parkin, G. *Chem. Rev.* **1993**, *93*, 887. (e) Rohmer, M.-M.; Bénard, M. *Chem. Soc. Rev.* **2001**, *30*, 340.

differ *only* in bond distances, in contrast with spin isomers¹⁵ that show differences in both bond distances and spin state.¹⁶ Furthermore, the term spin isomerism explicitly points to important differences in electronic structure and, consequently, color and magnetic properties. Even if the actual characterization of bond stretch isomerism is still a matter of debate, one can conceive the existence of isomers that differ in bond distances, while having the same spin state, as in the case of two differently Jahn–Teller-distorted Cu^{II} complexes reported by Comba and co-workers.¹⁷ Although those compounds have only been isolated in one of the isomeric forms, depending on some ligand substituents, they point to the existence of two different molecular configurations that could appropriately be termed bond-stretch isomers.

To characterize the stereochemistry of every theoretically optimized or experimentally determined molecular structure, we use, in the present study, Avnir's continuous shape measures and their associated parameters. The continuous shape measures (CShM)¹⁸ calibrate how close is a group of atoms Q (e.g., the metal and donor atoms in a coordination compound) to a given reference shape P , through the minimal distances between the equivalent atomic positions in the two structures, q_k (eq 1, where N is a normalization factor that makes the CShM values size independent).¹⁹ For the present study, we can compare metal coordination spheres with the regular tetrahedron and the square by means of the corresponding shape measures, $S(T)$ and $S(SP)$. A zero value of $S(T)$, for instance, indicates a perfectly tetrahedral geometry, while increasing values of this parameter reflect increasing distortions from the tetrahedron.

$$S_p(Q) = \frac{\sum_{k=1}^N q_k^2}{N} 100 \quad (1)$$

As an example, consider the two molecules of the [CuBr₄]²⁻ anion with different geometries shown in Figure 1. The shape measures of the molecule at the left relative to the square and to the tetrahedron are $S(SP) = 0.00$ and $S(T) = 32.06$, respectively, indicating that it has a perfectly square shape but is far from being tetrahedral. In contrast, the corresponding shape measures for the molecule at the right are 15.35 and 4.48, telling us that it is much closer to the tetrahedron than to the square, but significantly distorted from the ideal shape.

When dealing with a structure Q that is intermediate between two polyhedra T and P , its geometry is best described by its position along the minimal distortion path

for the interconversion of the two polyhedra. This can be done with the *generalized polyhedral interconversion coordinate*, $\varphi_{T \rightarrow P}^Q$,²⁰ derived from the shape measure of structure Q relative to the initial shape of the path, T , according to eq 2, where θ_{TP} is a constant characteristic of reference shapes T and P . When the structure is coincident with T , $\varphi_{T \rightarrow P}^Q$ is zero, while for a structure coincident with the end point of the path P , it amounts to 100%. Structures along the path have intermediate $\varphi_{T \rightarrow P}^Q$ values that correspond to the portion of the path covered (in percentage). In the case of the approximately tetrahedral [CuBr₄]²⁻ anion (Figure 1), the generalized coordinate calculated from eq 2 is $\varphi_{T \rightarrow P}^Q = 35\%$, indicating that the distortion from the tetrahedron is roughly one-third of that required to convert it into a square.

$$\varphi_{T \rightarrow P}^Q = \frac{100}{\theta_{TP}} \arcsin \left(\frac{\sqrt{S_Q(T)}}{10} \right) \quad (2)$$

To describe a structure according to its position along the tetrahedron–square interconversion path, we must make sure that it is really along that path. This can be done by calculating the *path deviation function* (eq 3), proposed previously by us,²¹ that measures how close (or how far) is the structure to the path. That function is zero for structures that fall exactly along the path and adopts increasing values as the structures are farther away from the path. The values of the path deviation function are given as percentages of the total length of the path. Thus, a deviation of a 100% indicates that the structure is at the same distance from the interconversion path as the two ideal polyhedra are from each other. For the present study, we will arbitrarily consider that all structures that deviate less than a 15% from the path can be approximately described by the generalized coordinate of eq 2.

$$\Delta_i(P, T) \equiv \frac{1}{\theta_{PT}} \left[\arcsin \sqrt{\frac{S_i(P)}{10}} + \arcsin \sqrt{\frac{S_i(T)}{10}} \right] - 1 \quad (3)$$

Stereochemical Preferences for Complexes with σ -Donor Ligands

To understand how the stereochemical preferences are affected by the number of valence electrons and the spin state, it is useful to have a Walsh diagram from which we can qualitatively deduce the preferred geometry for each electron configuration. For subsequent discussions based on the Walsh diagram, it is important to identify the d orbitals in a coordinate system that facilitate the understanding of changes in overlap and energy that accompany the geometry changes, for example, between the square planar and tetrahedral shapes. The typical composition of the d block orbitals and their approximate energy sequence are shown in Figure 2 for the sawhorse, tetrahedral, and square planar geometries. In what follows, we combine the qualitative picture provided by the Walsh diagram with the quantitative results of our geometry optimization for model complexes

(15) McGrady, J. *Angew. Chem., Int. Ed.* **2000**, *39*, 3077.

(16) (a) Gütllich, P.; Goodwin, H. A., Eds. *Spin Crossover in Transition Metal Compounds I*; Springer: Berlin, 2004; Vol. 233. (b) Gütllich, P.; Goodwin, H. A., Eds. *Spin Crossover in Transition Metal Compounds II*; Springer: Berlin, 2004; Vol. 234.

(17) Comba, P.; Hauser, A.; Kerscher, M.; Pritzkow, H. *Angew. Chem., Int. Ed.* **2003**, *42*, 4536.

(18) (a) Zabrodsky, H.; Peleg, S.; Avnir, D. *J. Am. Chem. Soc.* **1992**, *114*, 7843. (b) Avnir, D.; Katzenelson, O.; Keinan, S.; Pinsky, M.; Pinto, Y.; Salomon, Y.; Zabrodsky Hel-Or, H. In *Concepts in Chemistry: A Contemporary Challenge*; Rouvray, D. H., Ed.; Research Studies Press Ltd.: Taunton, U.K., 1996.

(19) Alvarez, S.; Alemany, P.; Casanova, D.; Cirera, J.; Llunell, M.; Avnir, D. *Coord. Chem. Rev.* **2005**, *249*, 1693.

(20) Cirera, J.; Ruiz, E.; Alvarez, S. *Chem.—Eur. J.* **2006**, *12*, 3162.

(21) Casanova, D.; Cirera, J.; Llunell, M.; Alemany, P.; Avnir, D.; Alvarez, S. *J. Am. Chem. Soc.* **2004**, *126*, 1755.

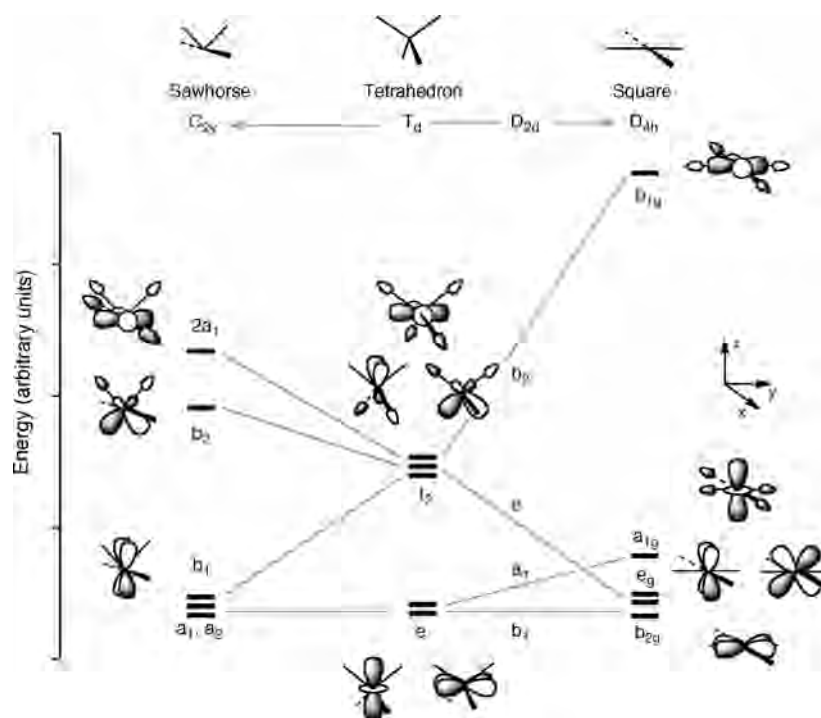


Figure 2. Walsh diagram for the d orbitals of a four-coordinate complex in sawhorse, tetrahedral, and square-planar geometries.

with σ -donor methyl ligands, considering as a starting point the tetrahedron.

A discussion of the d-orbital Walsh diagram for the conversion of tetrahedral to square planar molecules without²² or with valence d orbitals can be found in the literature,²³ but we consider also, in addition to those two geometries, a sawhorse structure that can be found for some electron configurations. While the ideal tetrahedral and square planar geometries are univocally determined by symmetry, our reference sawhorse geometry is arbitrarily taken as that of an octahedron with two cis coordination positions vacant. The Walsh diagram presented, intended to be used as a qualitative guide to understand the results of our DFT calculations, is based on extended Hückel calculations²⁴ for a metal atom with σ -donor only ligands. However, we have verified that such a Walsh diagram correctly represents the evolution of the orbital energies in density functional calculations, by comparison with the evolution of the Kohn–Sham orbital energies along the tetrahedron-square path for the cases of $[\text{TiMe}_4]$, $[\text{Ti}(\text{NH}_3)_4]^{2+}$, $[\text{MnMe}_4, S = 5/2]^{2-}$, and $[\text{ZnMe}_4]^{2-}$.

To discuss the expected stereochemistry for each d^n complex in its different spin states, we found it useful to classify all the spin configurations in three families, according to the mode of occupation of the t_2 orbitals in a hypothetical tetrahedral geometry. The reason for that choice is that the e orbitals are metal–ligand non-bonding, as far as only σ -interactions are considered, and changes in their occupation

have little effect on the stereochemistry of the metal center. In contrast, an uneven occupation of the t_2 orbitals gives rise to different Jahn–Teller distortions depending on the distribution of electrons within that orbital set. These are the three families of electron configurations we consider: (A) All three t_2 orbitals have the same number of electrons; (B) one of the t_2 orbitals has a higher occupation than the other two, and (C) one of the t_2 orbitals has a lower occupation than the other two. The spin configurations will be expressed in the form (ab/rst) , where a and b indicate the occupations of the two e orbitals, while those of the t_2 orbitals are represented by r , s , and t . The orbital occupations can go from 0 to 2 and, since we are interested only in the lowest energy state with a given spin, are constrained by the relationship $a \geq b \geq r \geq s \geq t$. As an example, for a d^4 complex, we will consider the following configurations: (22/000), (21/100), and (11/110).

A. Homogeneous Occupation of t_2 Orbitals. Let us consider here those spin configurations in which all the t_2 orbitals have identical occupation, that is, (ab/rrr) configurations, with $a \geq b \geq r$. First of all, we devote our attention to the electron configurations, in which the d shell is either completely empty or fully occupied. The results of our calculations on the d^0 complex $[\text{TiMe}_4]$ (Table 1) tell us that the tetrahedral structure is preferred in the absence of d electrons, while a frozen square planar geometry is some 70 kcal/mol higher in energy. A similar result is found for a d^{10} complex, $[\text{ZnMe}_4]^{2-}$. Indeed, in the tetrahedral geometry, the metal atom in d^0 and d^{10} complexes makes use of its valence s and p orbitals for σ bonding, that is, they employ a formal sp^3 hybridization in the valence-bond language, while the t_2 -type d orbitals are made formally non-bonding through mixing with the p orbitals, as schematically illustrated in Figure 2.¹²

(22) Gimarc, B. M. *Molecular Structure and Bonding*; Academic: New York, 1979.

(23) Albright, T. A.; Burdett, J. K.; Whangbo, W.-H. *Orbital Interactions in Chemistry*; J. Wiley: New York, 1985.

(24) (a) Hoffmann, R. *J. Chem. Phys.* **1963**, *39*, 1397. (b) Hoffmann, R.; Lipscomb, W. N. *J. Chem. Phys.* **1962**, *36*, 2179. (c) Hoffmann, R.; Lipscomb, W. N. *J. Chem. Phys.* **1962**, *37*, 2872.

Table 1. Shape Measures and Interconversion Coordinates of Optimized Model Methyl Complexes with Electron Configurations in which the t_2 Orbitals Are Homogeneously Occupied (Case A)^a

NVE	compd	config	$S(T)$	$S(SP)$	φ_{T-SP} (%)
d ⁰	[Ti ^{IV} Me ₄ , $S = 0$]	(00/000)	0.00	33.32	0
d ¹	[V ^{IV} Me ₄ , $S = 1/2$]	(10/000)	0.11	31.85	5
d ²	[Cr ^{IV} Me ₄ , $S = 1$]	(11/000)	0.00	33.31	0
d ²	[Cr ^{IV} Me ₄ , $S = 0$]	(20/000)	0.48	30.34	11
d ³	[V ^{II} Me ₄ , $S = 1/2$] ²⁻	(21/000)	0.00	33.27	0
d ⁴	[Mn ^{III} Me ₄ , $S = 0$] ⁻	(22/000)	0.00	33.26	0
d ⁵	[Mn ^{III} Me ₄ , $S = 5/2$] ²⁻	(11/111)	0.00	33.26	0
d ⁶	[Fe ^{II} Me ₄ , $S = 2$] ²⁻	(21/111)	0.07	31.82	4
d ⁷	[Co ^{II} Me ₄ , $S = 3/2$] ²⁻	(22/111)	0.00	33.27	0
d ¹⁰	[Zn ^{II} Me ₄ , $S = 0$] ²⁻	(22/222)	0.00	33.30	0

^a NVE is the number of valence d electrons; $S(T)$ and $S(SP)$ are the tetrahedral and square shape measures, respectively and φ_{T-SP} is the generalized interconversion coordinate.

Table 2. Shape Measures of Optimized Structures of Methyl Complexes with Electron Configurations with Higher Occupation of One of the t_2 Orbitals (Case B)^a

NVE	compd	config	$S(T)$	$S(SP)$	$S(SS)$	φ_{T-SP} (%)
d ³	[V ^{II} Me ₄ , $S = 3/2$] ²⁻	(11/100)	6.33	13.13	3.17	41
d ⁴	[Mn ^{III} Me ₄ , $S = 1$] ⁻	(21/100)	7.53	12.07	2.60	45
d ⁵	[Mn ^{II} Me ₄ , $S = 1/2$] ²⁻	(22/100)	26.20	0.62	13.98	87
d ⁶	[Fe ^{II} Me ₄ , $S = 0$] ²⁻	(22/200)	12.02	8.42	2.88	58
d ⁸	[Ni ^{II} Me ₄ , $S = 1$] ²⁻	(22/211)	1.50	25.47	3.95	20

^a NVE is the number of d electrons; the electron configuration given corresponds to the tetrahedral geometry; $S(T)$, $S(SP)$ and $S(SS)$ are the tetrahedral, square, and sawhorse shape measures, respectively; φ_{T-SP} is the generalized interconversion coordinate; and numbers in boldface indicate the closest ideal shape.

If we consider now electron configurations in which only the e orbitals are occupied, the preference for the tetrahedron is kept, since these orbitals are non-bonding for σ -donor ligands. This is the situation for the d¹, d² (in both the $S = 0$ and 1 states), d³ ($S = 1/2$), and d⁴ ($S = 0$) configurations, as seen in Table 1. For the d² case, the low-spin state that implies spin pairing of the two electrons within a set of degenerate orbitals is forbidden by Hund's rule and appears at high energy (see Supporting Information for the relative energies of optimized structures).¹² In addition, configurations in which the three t_2 orbitals are singly occupied also present a tetrahedral geometry because distortions result in roughly the same amount of stabilization and destabilization of the t_2 electrons (Figure 2). This is the case for d⁵ ($S = 5/2$), d⁶ ($S = 2$), d⁷ ($S = 3/2$), and d¹⁰ electron configurations, as confirmed by the geometry optimizations of the corresponding methyl complexes (Table 1). In summary, all the configurations in which the t_2 orbitals are equally occupied form a family for which a tetrahedral stereochemistry must be expected, as reflected by tetrahedral shape measures of less than 0.50, corresponding to planarization distortions of at most an 11%. The small deviations from a perfect tetrahedron are associated to a weak Jahn–Teller effect involving the non-bonding e orbitals.

B. Higher Occupation of One t_2 Orbital. We turn now to configurations that present an inhomogeneous occupation of the t_2 orbital set and look first at those in which one of those orbitals has a higher occupation than the other two, that is, (*ab/rss*) configurations with $a \geq b \geq r \geq s$. For those cases, the Jahn–Teller theorem makes us expect distortions from the ideal tetrahedral geometry. The Walsh diagram (Figure 2) shows that distortion toward a square planar

Table 3. Shape Measures and Related Magnitudes for the Optimized Geometries of Methyl Complexes Having Electron Configurations with One t_2 Orbital Less Occupied than the Other Two (Case C)^a

NVE	compd	config	$S(T)$	$S(SP)$	φ_{T-SP} (%)
d ⁴	[Mn ^{III} Me ₄ , $S = 2$] ⁻	(11/110)	18.64	2.83	72
d ⁵	[Mn ^{II} Me ₄ , $S = 3/2$] ²⁻	(21/110)	28.81	0.24	92
d ⁶	[Fe ^{II} Me ₄ , $S = 1$] ²⁻	(22/110)	33.34	0.01	100
d ⁷	[Co ^{II} Me ₄ , $S = 1/2$] ²⁻	(22/210)	27.67	0.38	90
d ⁸	[Ni ^{II} Me ₄ , $S = 0$] ²⁻	(22/220)	33.33	0.00	100
d ⁹	[Cu ^{II} Me ₄ , $S = 1/2$] ²⁻	(22/221)	12.15	6.58	58

^a NVE is the number of d electrons; $S(T)$ and $S(SP)$ are the tetrahedral and square shape measures, respectively; and φ_{T-SP} (%) is the generalized interconversion coordinate.

structure stabilizes two and destabilizes one of the t_2 orbitals, whereas the opposite occurs for the distortion toward a sawhorse. The preferred distortion, then, is the one that stabilizes those orbitals with higher occupation and destabilizes the ones with lower occupation. Hence, for the configurations considered here, we would predict a distortion toward a C_{2v} sawhorse structure. Consistently, the optimized geometries for those electron configurations deviate in all cases from the tetrahedron (Table 2). Some of them are best described as sawhorses, as in the cases of the d³, d⁴, and d⁶ complexes (Table 2 and Figure 3), although none of them deviates more than a 6% from the interconversion path between the tetrahedron and the square. The d⁵ stereospinomer [MnMe₄, $S = 1/2$]²⁻ is still more severely distorted, reaching a nearly planar structure (Figure 3), which is nevertheless along the square-sawhorse minimal distortion path (path deviation function = 2.3%). It is worth noting that for [FeMe₄, $S = 0$]²⁻, a second minimum with an umbrella distortion (three C–Fe–C bond angles of 124°) has also been characterized.

C. Lower Occupation of One t_2 Orbital. Finally, we are left with those configurations in which one of the t_2 orbitals has a lower occupation than the other two, of the type (*ab/rst*), with $a \geq b \geq r \geq s > t$. A look at Figure 2 tells us that, in such a case, one should expect the tetrahedron to distort toward the square, following the *spread* or planarization pathway. In four cases, the optimized structures (Table 3) are practically square planar, and the other two present high degrees of planarization. The least planar geometry corresponds to the d⁹ configuration of Cu^{II}, for which partial occupation of the highest d orbital prevents the distortion from going all the way toward the square, resulting in a geometry intermediate between the tetrahedron and the square. This situation, on the other hand reflects the well-known tendency of four-coordinate Cu^{II} complexes to present such intermediate geometries.² It must be stressed that in all these configurations the optimized structures fall precisely along the tetrahedron–square interconversion path, as indicated by the corresponding path deviation functions (not shown).

Preferred Stereospinomers and Experimental Structures for dⁿ Configurations

In a preliminary communication,²⁰ we have shown how the distribution of the experimental structures of d⁶ four-coordinate complexes along the interconversion path between

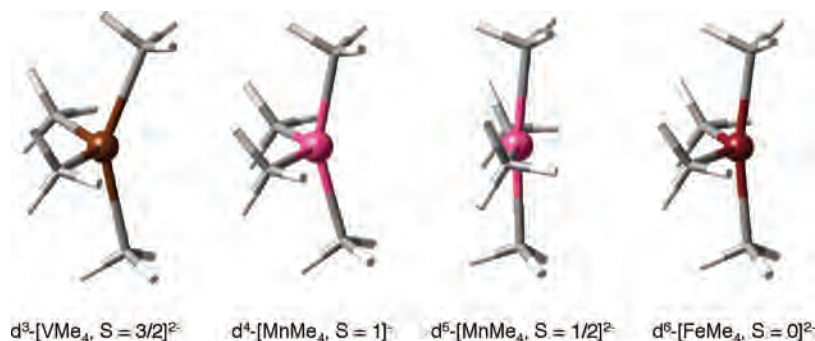


Figure 3. Optimized structures for some methyl complexes in configurations with higher occupation of one of the three t_2 orbitals (case B) and geometries distorted toward a sawhorse.

the tetrahedron and the square mirrors the shapes of the potential energy surfaces of two spin states ($S = 2$ and 1). In this section, we will show cross sections of the potential-energy surfaces, along the same path for each spin state of all d^n configurations in homoleptic methyl complexes. Then we will address the following question: do the calculations based on those simple complexes reasonably represent the stereochemical behavior of the variety of compounds with σ -donor ligands? To answer this question, we will look at the experimentally determined stereoisomers for a wide variety of homoleptic complexes with σ donor or π -acceptor ligands. Let us point out that the model compounds used in our calculations so far are restricted by the following criteria: (a) a “low” metal oxidation state (+2 or +3) whenever more than one spin state is possible, (b) σ -donor ligands only, and (c) metals of the first transition series. The discussion of the spin and stereochemistries of complexes with π -donor ligands, with higher oxidation states or with heavier metals (second or third transition series) is deferred to later sections.

To facilitate the discussion of the relative energy of different spin states while at the same time covering the structural variation, we have chosen to calculate the energy of each model complex along the interconversion pathway between the tetrahedron and the square. This has been done by fixing the dihedral angle between two MC_2 planes and reoptimizing at each point the geometry of the methyl groups and the $M-Me$ bond distances. The position of each such geometry along the interconversion path will be represented by the generalized interconversion coordinate φ_{T-SP} discussed above. For simplicity, we start with a group of electron configurations that have only one spin multiplicity: d^0 , d^1 , d^9 , and d^{10} .

d^0 , d^1 , d^9 , and d^{10} Configurations. The cross sections of the potential energy surfaces for these configurations along the planarization pathway are presented in Figures 4 and 5. For the d^0 configuration the energy minimum appears at the tetrahedral structure, as found in the full optimization (Table 1), and the energy increases steeply as we move toward the square. We should therefore expect the experimental structures for this configuration to be all very close to the tetrahedron, as actually found for a well-characterized homoleptic compound (Table 4) that shows a rather small deviation from the tetrahedron. Related mixed σ -donor ligand

complexes,²⁵ $[Ti(Si\{SiMe_3\}_3)(CH_2SiMe_3)_3]$, and $[Ti(Si\{SiMe_3\}_3)(CH_2^tBu)_3]$ are also slightly distorted tetrahedral ($\varphi_{T-SP} \approx 13\%$). A similar situation results for the d^1 configuration, although a weak Jahn–Teller distortion is expected (Table 1) that neatly shows up in the three characterized structures with this configuration (Table 4).

For the d^9 configuration (Figure 5), the situation is quite different, as expected from the above discussion based on the Walsh diagram (Table 3). In this case, not only the optimum structure is in-between the tetrahedron and the square but also the potential energy surface is very shallow, and the other geometries are not significantly higher in energy. Therefore, we should not expect a clear stereochemical preference for d^9 compounds. Consistently, homoleptic d^9 complexes show a variety of experimental structures between tetrahedral and square planar (Table 4).

Finally, the d^{10} configuration (Figure 5) is expected from the calculations to give essentially tetrahedral complexes. All structurally characterized homoleptic complexes with this electron configuration (Table 4) appear to be nearly perfect tetrahedra, the most distorted one being $[Ni(PMePh_2)_4]$,²⁶ with a distortion of a 17% toward the square. A remarkable exception is the highly distorted tetrahedral structure of the $[CuD_4]^{3-}$ anion²⁷ in $Ba_7(CuD_4)_3 \cdot D_5$ ($\varphi_{T-SP} = 30\%$) that results in a surprisingly short D–D distance worthwhile of a deeper structural investigation.

(25) McAlexander, L. H.; Hung, M.; Li, L.; Diminnie, J. B.; Xue, Z.; Yap, G. P. A.; Rheingold, A. L. *Organometallics* **1996**, *15*, 5231.

(26) Krieger, M.; Gould, R. O.; Harms, K.; Greiner, A.; Dehnicke, K. Z. *Anorg. Allgem. Chem.* **2001**, *627*, 747.

(27) Huang, B.; Fauth, F.; Yvon, K. *J. Alloys Compd.* **1996**, *244*, L1.

(28) Ara, I.; Forniés, J.; García-Monforte, M. A.; Martín, A.; Menjón, B. *Chem.–Eur. J.* **2004**, *10*, 4186.

(29) Alonso, P. J.; Forniés, J.; García-Monforte, M. A.; Martín, A.; Menjón, B. *Chem. Commun.* **2002**, 728.

(30) Glowiak, T.; Grobelny, R.; Jezowska-Trzebiatowska, B.; Kreisler, G.; Seidel, W.; Uhlig, E. *J. Organomet. Chem.* **1978**, *155*, 39.

(31) Bochmann, M.; Hawkins, I.; Hursthouse, M. B.; Short, R. L. *J. Organomet. Chem.* **1987**, *332*, 361.

(32) (a) Tebbe, K. F. *Z. Anorg. Allgem. Chem.* **1982**, *489*, 93. (b) Suzuki, S.; Morita, Y.; Fukui, K.; Sato, K.; Shiomi, D.; Takui, T.; Nakasuji, K. *Inorg. Chem.* **2005**, *44*, 8197.

(33) Gouteron, J.; Jeannin, S.; Jeannin, Y.; Livage, J.; Sanchez, C. *Inorg. Chem.* **1984**, *23*, 3387.

(34) Babich, O. A.; Kokozei, V. N.; Pavlenko, V. A. *Russ. J. Inorg. Chem.* **1996**, *41*, 74.

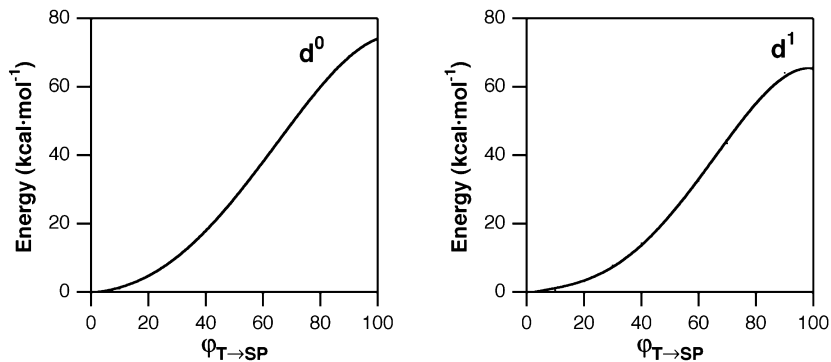


Figure 4. Calculated potential energy along the planarization pathway for d^0 -[TiMe₄] (left) and d^1 -[VMe₄] (right) complexes.

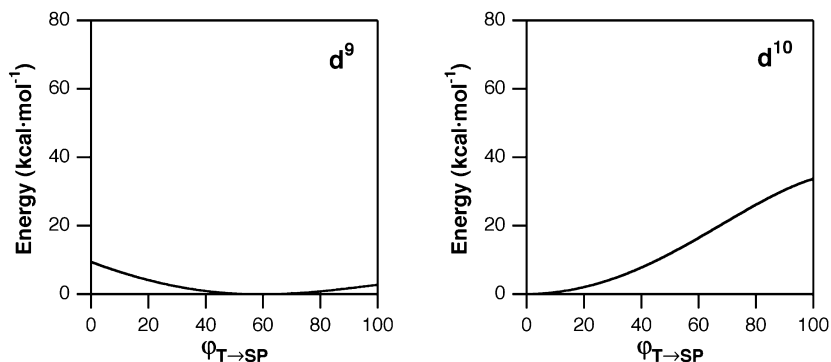


Figure 5. Calculated potential energy along the planarization pathway for d^9 -[CuMe₄]²⁻ (left) and d^{10} -[ZnMe₄]²⁻ (right) complexes with σ -donor ligands only.

Table 4. Experimental Geometries of Homoleptic Complexes of First Transition Series Metals with σ -Donor or π -Acceptor Ligands and Electron Configurations d^0 , d^1 , d^9 , or d^{10}

config	metal	ligand	geometry ^a	$\varphi_{T \rightarrow SP}(\%)^b$	ref
d^0	Ti ^{IV}	C ₆ Cl ₅	T	8	28
d^1	Ti ^{III}	C ₆ F ₅	T	16	29
	Ti ^{III}	C ₆ Cl ₅	T	16	29
d^9	V ^{IV}	Me ₃	T	18	30
	Ni ^I	PMe ₃	T	0	31
	Cu ^{II}	NH ₃	SP	100	32
	Cu ^{II}	NH ₂ Cy	int.	60	33
	Cu ^{II}	NH ₂ Me	SP	100	34
	Cu ^{II}	Me _n Im	SP	93–100	35
	Cu ^{II}	succinimidato	SP	61–100	36
	Cu ^{II}	NCS	int.	40	37
	Cu ^{II}	NH=SPH ₂	int.	45–100	35
	Cu ^{II}	N ₃	SP	100	38
d^{10}	Ni ⁰	H	T	6–11	39
	Ni ⁰	PEt ₃	T	6	40
	Ni ⁰	PMePh ₂	T	17	26
	Cu ^I	H	T	30	27
	Cu ^I	PMe ₃	T	0–4	35
	Cu ^I	PPh ₃	T	0–2	41
	Cu ^I	py	T	0	42
	Zn ^{II}	H	T	2–3	43
	Zn ^{II}	NH ₃	T	2–7	44
	Zn ^{II}	Me	T	6	45

^a T = tetrahedral, SP = square planar, int. = intermediate. ^b Ranges of the generalized coordinates given when several structures of the same complex ion exist.

d^2 Configuration. The potential energy curves for the two possible spin states (Figure 6) reflect the fact that the low-spin configuration ($S = 0$) is forbidden by Hund's rule for the d^2 metals because there are at least two nearly degenerate non-bonding d orbitals throughout the planarization path (Figure 2). Therefore, the stereospinomer with $S = 1$, and tetrahedral geometry is expected to be the only isolable

one. The experimental structures (Table 5) seem to confirm such a prediction. Even the coordination sphere of [Cr(CH₂SiMe₃)₄],⁴⁶ in which each donor atom is disordered into two positions, adapts well to the expected tetrahedral geometry if the centroid of each pair of positions is taken as the attachment point to the metal. A still smaller deviation from the tetrahedron (0.08) is found if only one of the two

- (35) Allen, F. H. *Acta Crystallogr.* **2002**, *B58*, 380.
 (36) (a) Tsukihara, T.; Katsube, Y.; Fujimori, K.; Kawashima, K.; Nanan, Y. *Bull. Chem. Soc. Jpn.* **1974**, *47*, 1582. (b) Tsukihara, T.; Katsube, Y.; Fujimori, K.; Ito, T. *Bull. Chem. Soc. Jpn.* **1972**, *45*, 2959.
 (37) Reinen, D.; Allmann, R.; Baum, G.; Kakob, B.; Kaschuba, U.; Massa, W.; Miller, G. J. *Z. Anorg. Allgem. Chem.* **1987**, *548*, 7.
 (38) (a) Saha, S.; Koner, S.; Tuchagues, J.-P.; Boudalis, A. K.; Okamoto, K.-I.; Banerjee, S.; Mal, D. *Inorg. Chem.* **2005**, *44*, 6379. (b) Woodward, B.; Willett, R. D.; Haddad, S.; Twamley, B.; Gómez-García, C. J.; Coronado, E. *Inorg. Chem.* **2004**, *43*, 1822. (c) Hiller, W.; Kosler, K.; Dehnicke, K. *Z. Anorg. Allgem. Chem.* **1989**, *574*, 7.
 (39) (a) Zolliker, P.; Yvon, K.; Jorgensen, J. D.; Rotella, F. J. *Inorg. Chem.* **1992**, *25*, 3590. (b) Kadir, K.; Noréus, D. *Inorg. Chem.* **2007**, *46*, 2220.
 (40) Hursthouse, M. B.; Izod, K. J.; Motevalli, M.; Thornton, P. *Polyhedron* **1994**, *13*, 151.
 (41) (a) Chi, K.-M.; Farkas, J.; Hampden-Smith, M. J.; Kostas, T. T.; Duesler, E. N. *J. Chem. Soc., Dalton Trans.* **1992**, 3111; (b) Engelhardt, L. M.; Pakawatchai, C.; White, A. H.; Healy, P. C. *J. Chem. Soc., Dalton Trans.* **1985**, 125.
 (42) Nilsson, K.; Oskarsson, A. *Acta Chem. Scand. A* **1982**, *36*, 605.
 (43) (a) Bortz, M.; Hewat, A. W.; Yvon, K. *J. Alloys Compd.* **1997**, *248*, 1. (b) Bortz, M.; Yvon, K.; Fischer, P. *J. Alloys Compd.* **1994**, *216*, 39.
 (44) (a) Guggenberger, L. *J. Inorg. Chem.* **1969**, *8*, 2771. (b) Klufers, P.; Wilhelm, U. *J. Organomet. Chem.* **1991**, *421*, 39. (c) Qu, Y.; Liu, Z.-D.; Tan, M.-Y.; Zhu, H.-L. *Acta Crystallogr.* **2004**, *E60*, m1343.
 (45) Weiss, E.; Wolfrum, R. *Chem. Ber.* **1968**, *101*, 35.
 (46) Schulzke, C.; Enright, D.; Sugiyama, H.; LeBlanc, G.; Gambarotta, S.; Yap, G. P. A.; Thompson, L. K.; Wilson, D. R.; Duchateau, R. *Organometallics* **2002**, *21*, 3810.

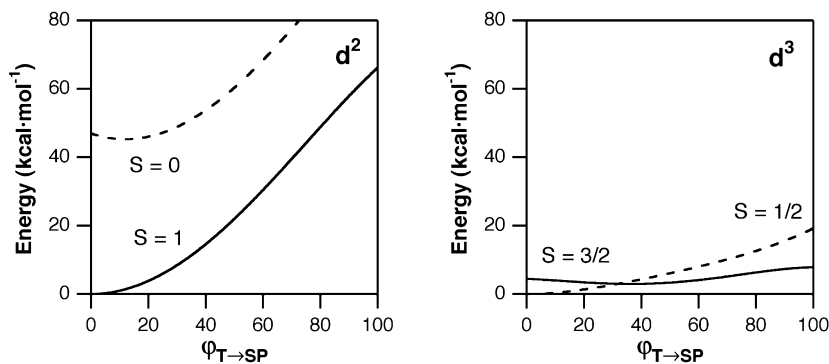


Figure 6. Calculated potential energy along the planarization pathway for d^2 -[CrMe₄] (left) and d^3 -[VMe₄]²⁻ (right) complexes.

Table 5. Experimental Geometry and Spin States for Homoleptic Complexes of First Transition Series Metals with σ -donor or π -acceptor Ligands and Electron Configurations d^2 , d^3 , and d^4

	metal	ligand	spin	geometry	$\varphi_{T \rightarrow SP}$ (%)	ref
d^2	Cr ^{IV}	C ₆ Cl ₃ H ₂	1	T	11	50
	Cr ^{IV}	Cy	1	T	7	51
	Cr ^{IV}	CH ₂ SiMe ₃	1	T	7 ^a	46
	Cr ^{IV}	CPh=CMe ₂	1	T	10	52
	V ^{III}	C ₆ Cl ₅	1	T	15	53
d^3	V ^{III}	C ₆ Cl ₃ H ₂	1	T		50
	Cr ^{III}	C ₆ Cl ₅	³ / ₂	int.	30	48
d^4	Cr ^{II}	Ph	2	SP	100	54
	Cr ^{II}	NCMe	2	SP	100	55
	Cr ^{II}	NCS	2	SP	100	56
	Cr ^{II}	2,5-Me ₂ pyrrolidyl	2	SP	76	57
	Cr ^{II}	Me	2	SP	100	58
	Cr ^{II}	C ₆ Cl ₅	2	SP	100	59
	Cr ^{II}	C ₆ F ₅	2	SP	100	60
	Cr ^{II}	NCMe	2	SP	100	55
	Mn ^{III}	Me	2	SP	74	67

^a The donor atoms are disordered over two positions; the generalized coordinate given corresponds to the centroid of the two positions for each ligand.

alternative positions is considered. Although the few examples found here correspond to the tetrahedral $S = 1$ stereospinomer, we will discuss elsewhere,⁴⁷ which conditions allow four-coordinate d^2 complexes to have a diamagnetic low-spin ground state.

d^3 Configuration. The full optimizations for this configuration predicted the low-spin state ($S = 1/2$) to be tetrahedral and the high-spin state ($S = 3/2$) to be distorted toward the sawhorse (Tables 1 and 2). However, the corresponding potential energy curves are rather flat and of similar energies (Figure 6), suggesting that a wide structural variability could be expected in either of the two spin states. Although we are aware of only one such homoleptic compound (Table 5), it presents a structure that is quite distant from both the tetrahedron and the square, consistent with the shape of the potential energy curve corresponding to the high-spin state (Figure 6, right) and with the optimized geometry for the isoelectronic V^{II} methyl complex (Table 2). That the d^3 methyl compound presents a coordination geometry similar to that experimentally reported for the [Cr(C₆Cl₅)₄]⁻ anion is an interesting observation because the presence of two intramolecular Cl...Cr contacts may suggest an effective pseudo-octahedral coordination.⁴⁸ Further confirmation of the

theoretical expectations is provided by the mixed-ligand complex [Cr(en)(CH₂Ph)(CHPh)], which is also found as an $S = 3/2$ square planar stereospinomer.⁴⁹

d^4 Configuration. For this configuration, three spin states can be foreseen. The optimized geometry for the lowest spin ($S = 0$) corresponds to a distorted tetrahedron (Table 1) that for the intermediate spin ($S = 1$) is closer to a sawhorse (Table 2), and the structure predicted for the highest spin ($S = 2$) is close to square planar (Table 3). In this case, though, the highest spin state is by far the most stable one. Such a result can be rationalized by taking into account that in both the tetrahedral low-spin and square planar high-spin situations the occupied d orbitals are essentially non-bonding (Figure 2), and exchange and interelectronic repulsion strongly disfavor the low-spin state. All the homoleptic compounds with this electron configuration appear consistently as the $S = 2$ square planar stereospinomer (Table 5), eventually with small deviations from that geometry, as for a Mn^{III} methyl complex⁶¹ ($\varphi_{T \rightarrow SP} = 74\%$), fully consistent with its most stable calculated stereospinomer (Table 3). Further examples can be found if we consider heteroleptic complexes that have been magnetically and structurally characterized. The examples found with σ -donor ligands appear in the $S = 2$ state with nearly square planar geometry ($73 < \varphi_{T \rightarrow SP} < 100\%$): [Cr(en)(CH₂Ph)₂],⁶¹ [Cr(en)(CH₂CMe₂Ph)],⁶¹ and [Cr(py)₂(2,5-Me₂pyrrolidyl)₂].⁵⁷

d^5 Configuration. The square planar geometry is the preferred one for the $S = 1/2$ and ³/₂ spin states of the d^5 configuration, but the $S = 5/2$ state appears to be more stable as a tetrahedron (Tables 1–3). It must be noticed, however, that for [MnMe₄]²⁻ the low-spin state ($S = 1/2$) is at quite high energy relative to the other two states (Figure 7). Although the tetrahedral $S = 5/2$ stereospinomer seems to

(49) Hao, S.; Song, J.-I.; Berno, P.; Gambarotta, S. *Organometallics* **1994**, *13*, 1326.

(50) García-Monforte, M. A. Ph.D. Thesis, Universidad de Zaragoza, Zaragoza, Spain, 2004.

(51) Stavropoulos, P.; Savage, P. D.; Tooze, R. P.; Wilkinson, G.; Hussain, B.; Motevalli, M.; Hursthouse, M. B. *J. Chem. Soc., Dalton Trans.* **1987**, 557.

(52) Cardin, C. J.; Cardin, D. J.; Kelly, J. M.; Norton, R. J.; Roy, A.; Hathaway, B. J.; King, T. J. *J. Chem. Soc., Dalton Trans.* **1983**, 671.

(53) Alonso, P. J.; Forniés, J.; García-Monforte, M. A.; Martín, A.; Menjón, B. *Chem. Commun.* **2001**, 2138.

(54) Edema, J. J. H.; Gambarotta, S.; van Bolhuis, F.; Smeets, W. J. J.; Spek, A. L.; Chiang, M. Y. *J. Organomet. Chem.* **1990**, *47*, 389.

(55) Henriques, R. T.; Herdtweck, E.; Kuhn, F. E.; Lopes, A. D.; Mink, J.; Romao, C. C. *J. Chem. Soc., Dalton Trans.* **1998**, 1293.

(56) Larkworthy, L. F.; Leonard, G. A.; Povey, D. C.; Tandon, S. S.; Tucker, B. J.; Smith, G. W. *J. Chem. Soc., Dalton Trans.* **1994**, 1425.

(47) Cirera, J.; Ruiz, E.; Alvarez, S. Unpublished work.

(48) Alonso, P. J.; Falvello, L. R.; Forniés, J.; García-Monforte, M. A.; Martín, A.; Menjón, B.; Rodríguez, G. *Chem. Commun.* **1998**, 1721.

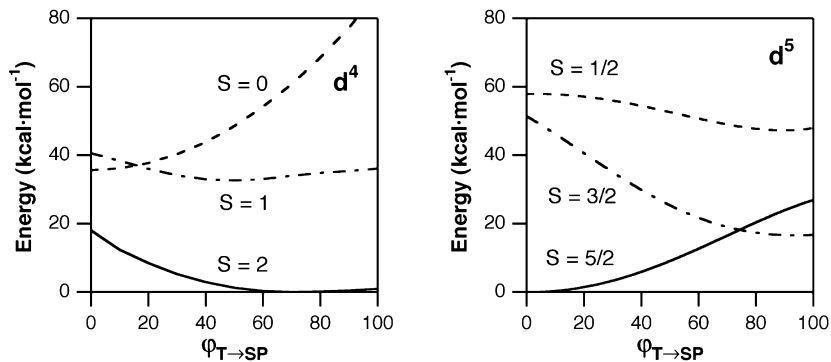


Figure 7. Calculated potential energy along the planarization pathway for d^4 -[MnMe₄]⁻ (left) and d^5 -[MnMe₄]²⁻ (right) complexes.

Table 6. Experimental Geometry and Spin States for Homoleptic d^5 and d^6 Complexes of First Transition Series Metals with σ -Donor or π -Acceptor Ligands

	metal	ligand	spin	geometry	$\phi_{T \rightarrow SP}$ (%)	ref
d^5	Mn ^{II}	Me	$5/2$	T	3	65
	Mn ^{II}	Et	$5/2$	T	6	66
	Mn ^{II}	C ₃ H ₁₁	$5/2$	T	2	66
	Mn ^{II}	H	$5/2$	T	6	67
	Mn ^{II}	H	$5/2$	T	2	67
	Mn ^{II}	H	$5/2$	T	3	67
	Mn ^{II}	CN	$5/2$	T	10	68
	Mn ^{II}	N ₃	$5/2$	T	25	69
	Fe ^{III}	C ₆ Cl ₅	$3/2$ - $5/2$	SP	84	62
	Co ^{IV}	Nor	$1/2$	T	5	70
d^6	Fe ^{II}	C ₆ F ₅	2	T	10	71
	Co ^{III}	C ₆ F ₅	1	SP		50

be more stable than the square planar $S = 3/2$ one, the difference in energy is not as large as to preclude that other combinations of metal and ligands could adopt this stereoisomeric form. As often happens with the d^5 configuration, the large number of exchange terms involved for five unpaired electrons favors the high-spin state, even if it requires to place three electrons in the higher energy t_2 orbital set. The experimental data (Table 6) seem to be consistent with the theoretical expectations because most structures are tetrahedral with $S = 5/2$. The only square planar d^5 complex studied from the point of view of its spin state⁶² that we are aware of has been explained as having an admixed ground state consisting of $S = 3/2$ and $5/2$ terms, the former being slightly lower in energy, a picture that nicely fits with the preferred tetrahedral shape for the $S = 3/2$ spin and the low energy of the higher spin configuration at that geometry (Figure 7). The only apparent contradiction with the qualitative expectations of the potential energy plot is provided by [Co(Nor)₄],⁶³ which presents a tetrahedral $S = 1/2$ stereoisomer, expected to be too high in energy compared with the other two stereoisomers (Figure 7). We note, however,

that the cobalt atom in that compound is in a higher oxidation state than considered in the model calculations. In a later section we will address the effect of a high-oxidation state on the potential energy surfaces presented in this section. Heteroleptic complexes with σ -donor ligands that have been magnetically and structurally characterized give the tetrahedral $S = 2$ stereoisomer, with varying degrees of distortion because of the different nature of the ligands or the presence of a bidentate ligand.⁶⁴

d^6 Configuration. As found above for the d^5 configuration, each of the three possible spin states of a d^6 complex should be expected to have a different coordination geometry: sawhorse ($S = 0$), square planar ($S = 1$), and tetrahedral ($S = 2$). Again, the low-spin state seems to be too high in energy, while the remaining two stereoisomers have comparable energies. Structural data for homoleptic complexes with this electron configuration (Table 6), even if scarce, are consistent with the predictions. Additional structural and magnetic data for some Fe^{II} mixed-ligand complexes with σ -donor ligands also correspond to either an $S = 2$ tetrahedral or an $S = 1$ square planar stereoisomer.⁷²

d^7 Configuration. The two alternative spin states of this configuration are expected to coexist with square planar ($S = 1/2$) and tetrahedral ($S = 3/2$) structures (Figure 8). Magnetostructural data found for homoleptic d^7 complexes (Table 7) are consistent with these predictions. The isolation of the two stereoisomers of Co^{II} complexes has been reported in a few cases.⁷³

(57) Edema, J. J. H.; Gambarotta, S.; Meetsma, A.; van Bolhuis, F.; Spek, A. L.; Smeets, W. J. J. *Inorg. Chem.* **1990**, *29*, 2147.

(58) Hao, S.; Gambarotta, S.; Bensimon, C. *J. Am. Chem. Soc.* **1992**, *114*, 3556.

(59) Alonso, P. J.; Forniés, J.; García-Monteforte, M. A.; Martín, A.; Menjón, B.; Rillo, C. *Chem.—Eur. J.* **2002**, *8*, 4056.

(60) Forniés, J.; Martín, A.; Martín, L. F.; Menjón, B.; Zhen, H.; Bell, A.; Rhodes, L. F. *Organometallics* **2005**, *24*, 3266.

(61) Morris, R. J.; Girolami, G. S. *Organometallics* **1991**, *10*, 792.

(62) Alonso, P. J.; Arauzo, A. B.; Forniés, J.; García-Monforte, M. A.; Martín, A.; Martínez, J. I.; Menjón, B.; Rillo, C.; Sáiz-Garaitaonandia, J. J. *Angew. Chem., Int. Ed.* **2006**, *45*, 6707.

(63) Byrne, E. K.; Theopold, K. H. *J. Am. Chem. Soc.* **1989**, *111*, 3887.

(64) (a) Muller, G.; Neugebauer, D.; Geike, W.; Kohler, F. H.; Pebler, J.; Schmidbaur, H. *Organometallics* **1983**, *2*, 257. (b) Howard, C. G.; Girolami, G. S.; Wilkinson, G.; Thornton-Pett, M.; Hursthouse, M. B. *J. Chem. Soc., Dalton Trans.* **1983**, 2631. (c) Hitchcock, P. B.; Lappert, M. H.; Leung, W.-P.; Buttrus, N. H. *J. Organomet. Chem.* **1990**, *394*, 57.

(65) Cotton, F. A.; Daniels, L. M.; Maloney, D. J.; Matonic, J. H.; Murillo, C. A. *Polyhedron* **1994**, *13*, 815.

(66) Morris, R. J.; Girolami, G. S. *Organometallics* **1989**, *8*, 1478.

(67) Bronger, W.; Hasenberg, S.; Auffermann, G. *J. Alloys Compd.* **1997**, *257*, 75.

(68) Buschmann, W. E.; Arif, A. M.; Miller, G. J. *Angew. Chem., Int. Ed.* **1998**, *37*, 781.

(69) Stenier, K.; Willing, W.; Muller, U.; Dehnicke, K. *Z. Anorg. Allgem. Chem.* **1987**, *555*, 7.

(70) Byrne, E. K.; Richeson, D. S.; Theopold, K. H. *Chem. Commun.* **1986**, 1491.

(71) Menjón, B.; Forniés, J. Personal communication.

(72) Hawrelak, E. J.; Bernskoetter, W. H.; Lbokovsky, E.; Yee, G. T.; Bill, E.; Chirik, P. J. *Inorg. Chem.* **2005**, *44*, 3103c.

(73) Goodwin, H. A. *Top. Curr. Chem.* **2006**, *234*, 23.

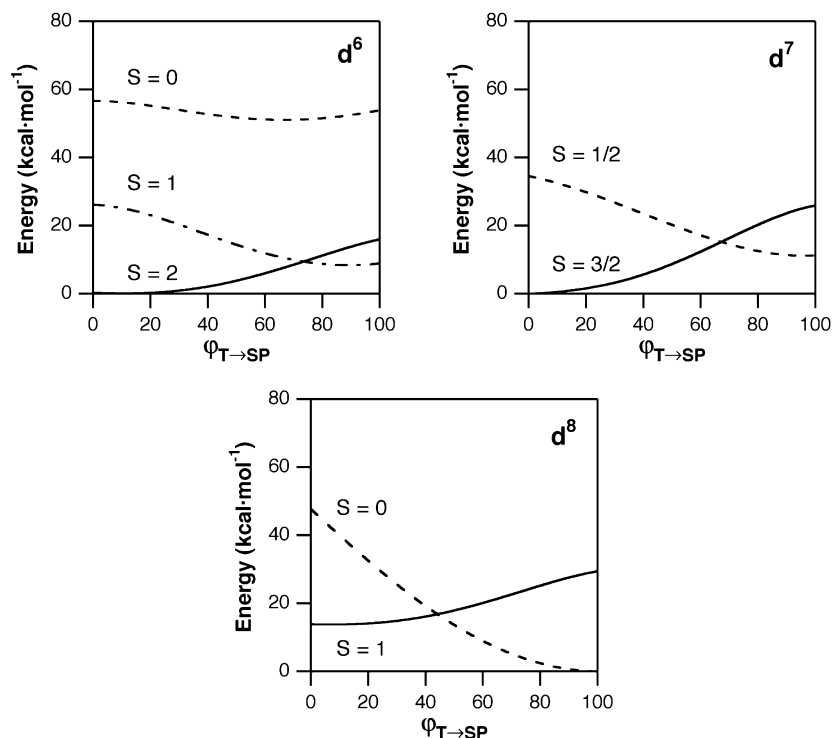


Figure 8. Calculated potential energy along the planarization pathway for d^6 -[FeMe₄]²⁻, d^7 -[CoMe₄]²⁻, and d^8 -[NiMe₄]²⁻.

Table 7. Experimental Geometry and Spin States of Homoleptic Complexes of First Transition Series Metals with Non- π -Donor Ligands and d^7 or d^8 Electron Configuration

	metal	ligand	spin	geometry	$\phi_{T \rightarrow SP}$ (%)	ref
d ⁷	Co ^{II}	C ₆ F ₅		SP	95	71
	Co ^{II}	CN	1/2	SP	100	75
	Co ^{II}	Im	3/2	T	6	76
	Co ^{II}	NCS	3/2	T	6	77
	Ni ^{III}	C ₆ Cl ₅	1/2	SP	89–98	78
d ⁸	Co ^I	PMe ₃	1	T	14	79
	Ni ^{II}	C ₆ F ₅		SP	94	71
	Ni ^{II}	CN	0	SP	100	35
	Ni ^{II}	C α CCN	0	SP	100	80
	Ni ^{II}	NCS	1	T	17	81
	Ni ^{II}	NH=C(Ar)NH ₂	0	SP	100	82
	Cu ^{III}	CHF ₂	0	SP	97	83

d⁸ Configuration. This is probably the best known case of stereospinomerism in transition metal chemistry, typically represented by the chemistry of Ni^{II} complexes. Of the two available options, the low-spin situation ($S = 0$) combines with a square planar geometry, and the high spin is predicted to be tetrahedral ($S = 1$). Although the square planar stereospinomer is calculated to be the ground state for our model compound, the tetrahedral one seems to be energetically accessible. Consistently, a few examples of each stereospinomer are found for homoleptic complexes (Table 7). Also the existence of the two energy minima is in keeping with the equilibrium between the two stereospinomers

observed for some Ni^{II} compounds.⁷⁴ It is interesting to observe that the energy minimum for the high-spin stereospinomer is relatively flat and centered away from the perfect tetrahedral shape, as found in the full optimization (Table 2). Consistently, and contrary to the general belief, the two homoleptic complexes that crystallize in this stereospinomeric form, [Ni(NCS)₄]²⁻ and [Co(PMe₃)₄]⁺, appear as distorted tetrahedra (Table 7) that could also be described as intermediate between the tetrahedron and the sawhorse.

General Trends. From the analysis of the different configurations, we can conclude that the high-spin stereospinomer is expected to be the most stable one for electron configurations with four to seven d electrons, and the low-spin one is preferred for the d^3 and d^8 configurations. Since the methyl ligands used in our calculations are strong field ligands,⁸⁴ we expect the high-spin preference of d^4 – d^7 ions to apply to most four-coordinate complexes of the first transition series with σ -donor ligands. How and why exceptions to these general rules can be expected will be the object of discussion in later sections.

If we consider those cases in which the topology of multidentate ligands imposes the shape of the coordination sphere, the calculated potential energy curves tell us which spin state should be expected for each d^n configuration. Thus, the tetrahedral geometry seems to favor, in all cases, the

(74) Holm, R. H. *Acc. Chem. Res.* **1969**, *2*, 307.

(75) Carter, S. J.; Foxman, B. M.; Stuhl, L. S. *J. Am. Chem. Soc.* **1984**, *106*, 4265.

(76) Tian, Y.-Q.; Cai, C.-X.; Ren, X.-M.; Duan, C.-Y.; Xu, Y.; Gao, S.; You, X.-Z. *Chem.—Eur. J.* **2003**, *9*, 5673.

(77) Drew, M. G. B.; Esho, F. S.; Nelson, S. M. *J. Chem. Soc., Dalton Trans.* **1983**, 1653.

(78) Alonso, P. J.; Falvello, L. R.; Forniés, J.; Martín, A.; Menjón, B.; Rodríguez, G. *Chem. Commun.* **1997**, 503.

(79) de Carvalho, L. C. A.; Dartiguenave, M.; Dartiguenave, Y.; Beauchamp, A. L. *J. Am. Chem. Soc.* **1984**, *106*, 6848.

(80) Zhou, Y.; Arif, A. M.; Miller, J. S. *Chem. Commun.* **1996**, 1881.

(81) Larue, B.; Tran, L.-T.; Luneau, D.; Reber, C. *Can. J. Chem.* **2003**, *81*, 1168.

(82) Guo, J.; Wong, W.-K.; Wong, W.-Y. *Eur. J. Inorg. Chem.* **2004**, 267.

(83) Eujen, R.; Hoge, B.; Brauer, D. J. *J. Organomet. Chem.* **1996**, *519*, 7.

(84) Chatt, J.; Hayter, R. G. *J. Chem. Soc.* **1961**, 772.

highest spin state, except maybe for the d^3 configuration. On the other hand, the square planar geometry also favors the highest spin for the d^2 – d^4 configurations, but the intermediate spin ($S = 3/2$) for d^5 and the low-spin state for the d^6 – d^8 ions. This is what is found for complexes of porphyrinato and related macrocyclic ligands (phthalocyaninato, porphyrinogens, or porphyrizinato), for which the square planar coordination geometry is imposed by the rigidity of the ligand and the metal ion appears in the expected spin state:⁸⁵ $S = 2$ for Cr^{II} , $S = 3/2$ for Mn^{II} and Fe^{III} , $S = 1$ for Co^{III} and Fe^{II} , $S = 1/2$ for Co^{III} , and $S = 0$ for Ni^{II} (see Supporting Information for more references, shape measures, and spin states of a variety of such compounds).

Forcing a tetrahedral coordination geometry seems more complicated and less productive. A look at Figures 6–8 tells us that the tetrahedron is already the preferred geometry in most cases. Therefore, the use of tridentate ligands such as tris(pyrazolyl)borate (abbreviated Tp in general, without mention to the different substituents present at the aromatic rings) in complexes of the type $[\text{TpM}^{\text{II}}\text{X}]$ or $[\text{TpM}^{\text{I}}\text{L}]$ for $\text{M} = \text{Mn}, \text{Fe}, \text{Co},$ or Ni , results in the tetrahedral high-spin stereospinomer⁸⁶ as predicted for the related complexes with monodentate ligands (Figures 6 and 7). Deviations from the ideal tetrahedral shape in those compounds are minor (shape measures $S(T) \leq 5.0$) and are caused by the small bond angles spanned by the tridentate ligand (between 84 and 100° for 83 structures found in the CSD). In contrast, the d^4 – $[\text{TpCr}^{\text{II}}\text{X}]$ complexes ($\text{X} = \text{Cl}, \text{Me}, \text{Ph}$),⁸⁷ appear in a sawhorse geometry (shape measures $S(SS) \leq 2.5$) with a high-spin state, in agreement with the potential energy curve (Figure 7) for the model complex with monodentate ligands that predicts the $S = 1$ state to be the most stable one with a non-tetrahedral structure. It must be pointed out, though, that a combination of tridentate ligands with small bite angles and a π -donor monodentate ligand may result in an unusual stereospinomer with pseudotetrahedral geometry and a low-spin state or even in spin-crossover behavior, as reported by Peters and co-workers⁸⁸ and discussed recently by ourselves in more detail.¹²

Agostic interactions⁸⁹ seem to appear in the optimized structures of some stereospinomers of $[\text{MMe}_4]$ complexes, as evidenced by a marked asymmetry in the $\text{M}-\text{C}-\text{H}$ bond angles, calibrated by the difference between the two larger and the smaller $\text{M}-\text{C}-\text{H}$ bond angles, δ . However, the strongest structural effects attributable to agostic interactions (δ values between 11 and 18°) do not correspond to the most stable stereospinomer. The most stable stereospinomers that present significant δ values are $[\text{VMe}_4, S = 1/2]^{2-}$, $\delta = 7^\circ$; $[\text{CrMe}_4, S = 2]^{2-}$, $\delta = 6^\circ$; $[\text{CoMe}_4, S = 1/2]$, $\delta = 11^\circ$; and $[\text{CuMe}_4]^{2-}$, $\delta = 6^\circ$. Further discussion of the reasons for the appearance of agostic interactions in the particular stereospinomers commented above is outside the scope of this work. We note, however, that agostic interactions detected at four-coordinate metal centers so far seem to correspond only to d^0 metal ions.⁹⁰

Effect of π -Donor Ligands

The potential energy curves for the methyl complexes discussed above provide a sound qualitative rationale for the stereospinomers found experimentally in homoleptic complexes with σ -donor ligands. However, the potential energy surfaces for complexes with ligands of weak σ -donor and strong π -bonding character might be significantly modified, as shown in our preliminary communication for the case of a d^6 ion.²⁰ Therefore, we have calculated potential energy profiles for all possible spin states of representative homoleptic complexes with π -donor ligands, of general formula $[\text{MCl}_4]^{n-}$. The potential energy curves (Figure 9 and Supporting Information) for the different electron configurations clearly show that the introduction of π -donor ligands significantly destabilizes the low-spin configuration relative to the high-spin one in all cases. Compare, for instance, the energy curves for the chloro complexes with d^4 and d^8 configurations (Figure 9) with those for the corresponding methyl complexes (Figures 7 and 8, respectively). The only

- (85) Scheidt, R. In *The Porphyrin Handbook*; Kadish, K. M., Smith, K. M., Guillard, R., Eds.; Academic Press: New York, 2000; Vol. 3, p 112.
- (86) (a) Detrich, J. L.; Konecny, R.; Vetter, W. M.; Doren, D.; Rheingold, A. L.; Theopold, K. H. *J. Am. Chem. Soc.* **1996**, *118*, 1703. (b) Jewson, J. D.; Liable-Sands, L. M.; Yap, G. P. A.; Rheingold, A. L.; Theopold, K. H. *Organometallics* **1999**, *18*, 300. (c) Uehara, K.; Hikichi, S.; Inagaki, A.; Akita, M. *Chem.—Eur. J.* **2005**, *11*, 2788. (d) Shirasawa, N.; Akita, M.; Hikichi, S.; Moro-oka, Y. *Chem. Commun.* **1999**, 417. (e) Shirasawa, N.; Nguyet, T. T.; Hikichi, S.; Moro-oka, Y.; Akita, M. *Organometallics* **2001**, *20*, 3582. (f) Yoshimitsu, S.; Hikichi, S.; Akita, M. *Organometallics* **2002**, *21*, 3762. (g) Brunker, T. J.; Hascall, T.; Cowley, A. R.; Rees, L. H.; O'Hare, D. *Inorg. Chem.* **2001**, *40*, 3170. (h) Schebler, P. J.; Mandimutsira, B. S.; Riordan, C. G.; Liable-Sands, L. M.; Incarvito, C. D.; Rheingold, A. L. *J. Am. Chem. Soc.* **2001**, *123*, 331. (i) DuPont, J. A.; Coxey, M. B.; Schebler, P. J.; Incarvito, C. D.; Dougherty, W. G.; Yap, G. P. A.; Rheingold, A. L.; Riordan, C. G. *Organometallics* **2007**, *26*, 971.
- (87) Kersten, J. L.; Kucharczyk, R. R.; Yap, G. P. A.; Rheingold, A. L.; Theopold, K. H. *Chem.—Eur. J.* **1997**, *3*, 1668.
- (88) (a) Brown, S. D.; Peters, J. C. *J. Am. Chem. Soc.* **2005**, *127*, 1913. (b) Jenkins, D. M.; Peters, J. C. *J. Am. Chem. Soc.* **2003**, *125*, 11162.

- (89) (a) Brookhart, M.; Green, M. L. H. *J. Organomet. Chem.* **1983**, *250*, 395. (b) Kubas, G. J. *Metal Dihydrogen and σ -Bond Complexes: Structure, Theory, and Reactivity*; Kluwer Academic Publishers: New York, 2001. (c) Clot, E.; Eisenstein, O. *Struct. Bonding (Berlin)* **2004**, *113*, 1.
- (90) Scherer, W.; McGrady, G. S. *Angew. Chem., Int. Ed.* **2004**, *43*, 1782.
- (91) Hoppe, R.; Mader, K. Z. *Anorg. Allgem. Chem.* **1990**, *586*, 115.
- (92) Jeannot, C.; Malaman, B.; Gerardin, R.; Oulladiad, B. *J. Solid State Chem.* **2002**, *165*, 266.
- (93) Delattre, J. L.; Stacy, A. M.; Young, V. G.; Long, G. J.; Hermann, R.; Grandjean, F. *Inorg. Chem.* **2002**, *41*, 2834.
- (94) Babar, M. A.; Ladd, M. F. C.; Larkworthy, L. F.; Povey, D. C.; Proctor, K. J.; Summers, L. J. *Chem. Commun.* **1981**, 1046.
- (95) Chan, J. Y.; Olmstead, M. M.; Kaulzarich, S. M. *Chem. Mater.* **1998**, *10*, 3583.
- (96) Kim, J.-Y.; Wang, C.-C.; Hughbanks, T. *Inorg. Chem.* **1999**, *38*, 235.
- (97) Fleischer, T.; Hoppe, R. Z. *Anorg. Allgem. Chem.* **1982**, *492*, 76.
- (98) Boudreaux, E. A.; Mulay, L. N. *Theory and Applications of Molecular Paramagnetism*; John Wiley & Sons: New York, 1976.
- (99) Hitchcock, P. B.; Lee, T. H.; Leigh, G. J. *Inorg. Chim. Acta* **2003**, *355*, 168.
- (100) von Schnering, H. G.; Kolloch, B.; Kolodziejczyk, A. *Angew. Chem.* **1971**, *83*, 440.
- (101) Bailloul, S.; Svoronos, D.; Porcher, P.; Tomas, A. C. R. *Hebd. Seances Acad. Sci., Ser. 2* **1991**, *313*, 1149.
- (102) Puget, R.; Jannin, M.; Perret, R.; Godefroy, L.; Godefroy, G. *Ferroelectrics* **1990**, *107*, 229.
- (103) *ICSD Database*; FIZ Karlsruhe: Karlsruhe, Germany, 2006.

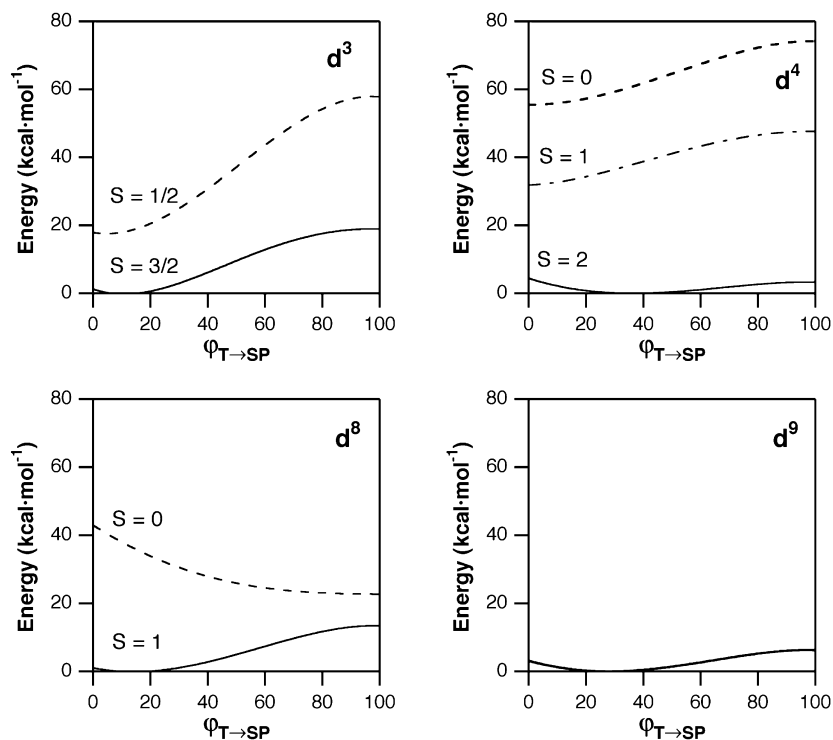


Figure 9. Potential energy curves along the tetrahedron–square interconversion path for d^3 -[VCl₄]²⁻, d^4 -[CrCl₄]²⁻, d^8 -[NiCl₄]²⁻ and d^9 -[CuCl₄]²⁻ complexes.

Table 8. Most Stable Stereospinomers for Model Complexes with π -Donor Ligands and Metal Ions of the First Transition Series^a

NVE	compd	config.	$S(T)$	$S(SP)$	$\varphi_{T\rightarrow SP}$ (%)
d ⁰	[TiCl ₄ , $S = 0$]	(00/000)	0.00	33.33	0
d ¹	[VCl ₄ , $S = 1/2$]	(10/000)	0.09	30.61	5
d ²	[CrCl ₄ , $S = 1$]	(11/000)	0.00	33.33	0
d ³	[VCl ₄ , $S = 3/2$] ²⁻	(11/100)	0.43	28.45	11
d ⁴	[CrCl ₄ , $S = 2$] ²⁻	(11/110)	5.11	14.28	37
d ⁵	[MnCl ₄ , $S = 5/2$] ²⁻	(11/111)	0.00	33.33	0
d ⁶	[FeCl ₄ , $S = 2$] ²⁻	(21/111)	0.08	31.78	5
d ⁷	[CoCl ₄ , $S = 3/2$] ²⁻	(22/111)	0.00	33.24	0
d ⁸	[NiCl ₄ , $S = 1$] ²⁻	(22/211)	0.28	30.04	9
d ⁹	[CuCl ₄ , $S = 1/2$] ²⁻	(22/221)	3.09	18.05	29
d ¹⁰	[ZnCl ₄ , $S = 0$] ²⁻	(22/222)	0.00	33.33	0

^a $S(T)$ and $S(SP)$ are the tetrahedral and square planar shape measures, respectively, and $\varphi_{T\rightarrow SP}$ (%) is the generalized interconversion coordinate between the tetrahedron and the square. Deviations from the minimum distortion path are in all cases less than a 2%.

configurations for which the tetrahedral geometry is not clearly favored are d^4 , d^8 , and d^9 (Figure 9).

The geometries of the [MCl₄]ⁿ⁻ complexes in their different spin states have been optimized and confirmed to correspond to energy minima through vibrational analysis (coordinates of optimized geometries provided as Supporting Information). The geometries of the high-spin ground states are summarized in Table 8 through the corresponding shape measures and generalized coordinates. A general trend that is found in the optimized geometries (Table 8) is that distortions predicted on the basis of the Jahn–Teller theorem appear for all configurations with inhomogeneous occupation of one set of degenerate orbitals (i.e., d^1 , d^3 , d^4 , d^6 , d^8 , and d^9), whereas those configurations with homogeneous occupation of degenerate orbitals are perfectly tetrahedral (d^0 , d^2 , d^5 , d^7 , and d^{10}). Furthermore, it can be seen that the degree of Jahn–Teller distortion varies according to the type of orbital configuration: (a) compounds in which the Jahn–Teller

effect is caused by the dissimilar occupation of the e orbitals (d^1 and d^6 configurations) present minor distortions (5% along the tetrahedron to square path), (b) whenever there is one t_2 orbital with a higher occupation than the other two (i.e., d^3 and d^8 configurations), a larger distortion ($\varphi_{T\rightarrow SP} \approx 10\%$) results, and (c) if two t_2 orbitals have higher occupation than the third one (d^4 and d^9 configurations), the distortion is severe ($\varphi_{T\rightarrow SP} \geq 29\%$).

From an analysis of the composition and energies of the molecular orbitals with major 3d contributions in the presence of π -donor ligands, we can attribute the higher stability of the high-spin tetrahedral stereospinomers to two factors: (a) a stronger ligand–ligand repulsion involving the ligands' π lone pairs in the square planar conformation and (b) a higher destabilization of the e set of d orbitals compared to the t_2 set in the tetrahedral case. Let us look first at the differences in ligand–ligand repulsion. On one hand, for the same metal–ligand distance, the ligand–ligand distance is significantly longer in the tetrahedral geometry (Figure 10). On the other hand, the relative orientation of the π lone pair orbitals favors a stronger overlap (hence a stronger repulsion between those electron pairs), both because of the smaller L–M–L bond angle and because each orbital interacts strongly with those of the two cis ligands in the same plane in the square, but with only one coplanar orbital in the tetrahedral one.

The second factor is illustrated with the topology of the calculated molecular orbitals shown in Figure 11, to be compared with the schematic drawings of Figure 2 for the σ -donor ligands. It can be seen that each t_2 orbital, bearing σ -antibonding interactions with two ligands, incorporates π -antibonding interactions with the other two ligands,

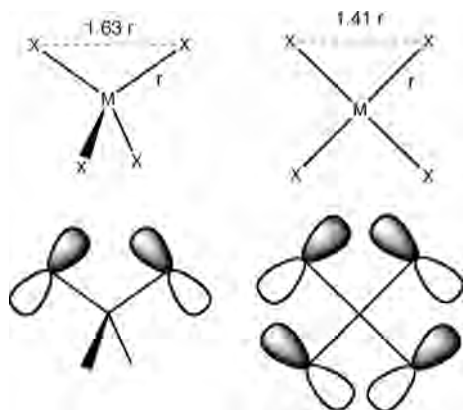


Figure 10. Differences in geometric (above) and orbital orientation (below) relationships between the tetrahedral and square planar geometries that result in stronger ligand–ligand repulsions in complexes with π -donor ligands for the latter.

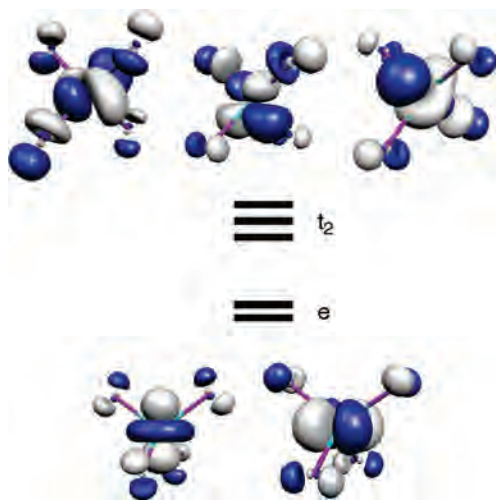


Figure 11. Isodensity surfaces for the d orbitals of $[\text{TiCl}_4]$ in its optimized structure, showing the π -antibonding contributions of two ligands to the t_2 orbital and of four ligands to the e orbitals.

resulting in an extra destabilization of these orbitals resulting from the π -donor nature of the ligands. However, the e orbitals, which are strictly non-bonding when the ligands are σ -donors only, incorporate π -antibonding interactions with all four ligands. Hence, the e orbitals are more destabilized than the t_2 ones by π -donor interactions, and the e– t_2 orbital gap is reduced. As a result, the high-spin states are favored in the presence of π -donor ligands.

Even if the stereochemical predictions for the $[\text{MCl}_4]^{n-}$ complexes (Table 9) are well understood, a straightforward extrapolation to all complexes with π -donor ligands should be made with care. It is thus important to take into account the shapes of the calculated potential energy profiles. In some cases, the steep nature of the potential energy well makes us expect that substitution of chlorides by other π -donor ligands should not significantly change the position of the energy minimum. This is the case of the tetrahedral geometry expected for d^0 , d^1 , d^2 , d^5 , and d^6 configurations and for the distorted tetrahedral geometry in d^7 complexes. In contrast, the shallow potential energy surfaces found for d^3 , d^4 , d^8 , and d^9 configurations make us think that different metals or ligands should be able to substantially modify the position

Table 9. Experimental Geometry and Spin States for Homoleptic Complexes of First Transition Series Metals with π -donor Ligands and d^3 , d^4 , d^8 , or d^9 Electron Configurations

	metal	ligand	spin	geometry ^a	$\varphi_{\text{T-SP}}$ (%)	ref
d^3	Fe ^V	O ²⁻	$3/2$	T	12	91
d^4	Fe ^{IV}	O ²⁻	2	T	23	92
	Fe ^{IV}	O ²⁻	2	T	21	93
	Fe ^{IV}	O ²⁻	2	T	3	93
d^8	Cr ^{II}	Cl ⁻	2	SP	100	94
	Mn ^{III}	Sb ³⁻	2	T	11	95
	Mn ^{III}	Te ²⁻	2	T	0.0	96
	Cu ^{III}	F ⁻	0	SP	100	97
d^9	Ni ^{II}	Cl ⁻	1	T	0–10	35, 98
	Ni ^{II}	Br ⁻	1	T	9	99
	Cu ^{II}	F ⁻	$1/2$	SP	100	100
d^9	Cu ^{II}	Cl ⁻	$1/2$	T	28	101
	Cu ^{II}	Br ⁻	$1/2$	T	27	102
	Cu ^{II}	Br ⁻	$1/2$	int.	15–100	35
	Cu ^{II}	Br ⁻	$1/2$	SP	98–100	103
	Cu ^{II}	O ²⁻	$1/2$	SP	98–100	103

^a T, SP, and int. indicate tetrahedral, square planar, and intermediate geometries, respectively, and $\varphi_{\text{T-SP}}$ (%) is the generalized interconversion coordinate between the tetrahedron and the square.

of the energy minimum and variable geometries should be expected.

A look at the magnetostructural data for four-coordinate complexes with first transition series metals and π -donor ligands (Table 9 for the d^3 , d^4 , d^8 , and d^9 configurations and Supporting Information for the rest of the d^n configurations) are consistent with the theoretical rules established above on the basis of our calculations on representative chloro complexes. Hence, all first transition series d^4 , d^5 , and d^6 complexes with π -donor ligands for which the magnetic behavior has been reported are in their high-spin configuration. Furthermore, the geometries of those complexes are also consistent with the rules discussed in the previous paragraph, as shown by their generalized interconversion coordinates (Table 9).

The only apparent contradiction between the structural data and the expected geometry corresponds to the $[\text{VO}_4]^{3-}$ anion of K_3VO_4 , which appears¹⁰⁴ as a significantly distorted tetrahedron along the planarization pathway ($\varphi_{\text{T-SP}} = 20\%$), while a perfectly tetrahedral geometry is expected for such a d^0 ion. We think that in this case the potassium host lattice is responsible for the distortion. In effect, the potassium and vanadium cations in this compound form a body-centered cubic structure analogous to that of metallic potassium, and the occupation of four interstitial sites around the cube center by O atoms in such a lattice¹⁰⁵ yields a flattened tetrahedral coordination, characterized by a 25% shift toward the square planar geometry. Occupation of those interstitial sites by the oxide ions is favored because in that way they become four-coordinated to one V^V and three K⁺ ions.

In this section, we have considered only monatomic ligands as π -donors, also termed *double-faced π -donors*¹⁰⁶ because each ligand carries one σ -lone pair and two lone pairs capable of π -interacting with the metal atom. *Single-faced π -donors* such as amides or thiolates, in contrast, have

(104) Olazcuaga, R.; Reau, J. M.; le Flem, G.; Hagenmüller, P. *Z. Anorg. Allgem. Chem.* **1975**, *412*, 271.

(105) (a) Barrett, C. S. *Acta Crystallogr.* **1956**, *9*, 671. (b) Liu, L.-G. *J. Phys. Chem. Solids* **1986**, *47*, 1067.

(106) Rossi, A. R.; Hoffmann, R. *Inorg. Chem.* **1975**, *14*, 365.

Table 10. Optimized Stereospinomers for d^3 – d^6 Complexes with σ -Donor Ligands and a High-Oxidation State^a

compd	config	spin	$S(T)$	$S(SP)$	φ_{T-SP} (%)	ΔE (kcal/mol)
[Mn ^{IV} Me ₄]	d ³	1/2	0.05	32.33	98	13.0
		3/2	3.06	26.38	<i>b</i>	0.0
[Fe ^{IV} Me ₄]	d ⁴	0	0.00	0.62	0	0.0
		2	5.95	13.02	40	5.7
[Co ^{IV} Me ₄]	d ⁵	1/2	3.12	26.86	29	0.0
		5/2	0.00	33.30	0	32.3
[Ni ^{IV} Me ₄]	d ⁶	0	6.54	25.14	<i>b</i>	0.0
		2	0.01	33.16	0	10.5

^a More details and information on the intermediate spin states provided as Supporting Information. ^b This stereospinomer deviates significantly from the tetrahedron-square interconversion path.

only one σ and one π lone pair available for bonding to a Lewis acid. For simplicity, a study of the stereochemical preferences of four-coordinate complexes with single-faced π -donors will be reported elsewhere.⁴⁷ Let us just mention here that such ligands have a differential behavior, in the sense that spin pairing in the lowest d orbital is favored, thus resulting in low-spin configurations for d^2 or d^3 complexes.

Effect of the Metal Oxidation State

Going back to the case of complexes with σ -donor ligands, we worry now about the effect of the metal oxidation state on the preferred stereospinomer. We have thus optimized several methyl complexes with the metal in its +4 oxidation state (Table 10) for those configurations for which a tetrahedral low-spin state could be expected if the d orbital splitting was large enough. We compare in this section these results with those obtained above for the isoelectronic analogues in a lower (+2) oxidation state (Tables 1–3). Such a comparison shows that the low-spin configuration is strongly stabilized and the corresponding stereospinomer becomes the most stable one except for the d^3 case. The behavior of the d^4 – d^6 configurations indicates that the high-oxidation state is responsible for a more covalent metal–ligand interaction and an enhanced d orbital splitting that favors the low-spin situation. However, the opposite trend found for the d^3 configuration suggests that such a splitting may not be large enough as to favor the low-spin state when the t_2 set (Figure 2) is occupied by only one electron.

To illustrate the effect of the oxidation state on the d orbital splitting, consider the Mn^{II} compound, for which the t_2 orbital set lies 17 000 cm^{-1} above the e set (Kohn–Sham orbital energies in the high-spin optimized structure), and the isoelectronic Co^{IV} complex with a gap 34 000 cm^{-1} , a value much closer to those found in high-field octahedral complexes than in tetrahedral ones.¹⁰⁷

The only four-coordinate homoleptic compound with a first transition series metal in an oxidation state higher than +3 and an electron configuration between d^3 and d^6 that we are aware of is [Co(Norbornyl)₄].⁶³ This compound appears as an $S = 1/2$ tetrahedral stereospinomer (Table 6), in excellent agreement with the results for the calculated [CoMe₄] complex (Table 10).

(107) Lever, A. B. P. *Inorganic Electronic Spectroscopy*; 2nd ed.; Elsevier: Amsterdam, 1984.

Table 11. Optimized Geometries and Relative Energies for the High- and Low-Spin Stereospinomers of d^4 Complexes of First and Second Transition Series Metals with Methyl Ligands

metal	spin	φ_{T-SP} (%) ^a	E (kcal/mol)
Cr ^{II}	2	90	0.0
	0	36	47.5
Mn ^{III}	2	72	0.0
	0	0	35.6
Fe ^{IV}	2	40	5.7
	0	0	0.0
Mo ^{II}	2	99	19.2
	0	14	12.2
Ru ^{IV}	2	44	56.2
	0	0	0.0

^a φ_{T-SP} is the generalized interconversion coordinate between the tetrahedron and the square. Deviations from the minimum distortion path are in all cases less than a 1%.

Heavier Transition Metals

It is well-known that the second and third series transition metals present both larger splitting of the d orbitals^{107,108} and a weaker interelectronic repulsion^{108,109} than the lighter member of the same periodic group with the same set of ligands. Consequently, one should expect the tetrahedral low-spin configuration to be more stable for the heavier transition metals. To learn how the relative energies of the different stereospinomers change as we descend down a group of the periodic table, we compare here the optimized structures of the low- and high-spin states of the d^4 complexes [MoMe₄]²⁻ and [RuMe₄] with those of the previously discussed isoelectronic first row analogues (Table 11).

Comparison of the results for the Cr^{II} and Mo^{II} complexes clearly show that the low-spin tetrahedral stereospinomer becomes more stable than the square planar high-spin one for the heavier metal, even if in this case the ground state is found to correspond to the intermediate spin state with a sawhorse geometry. The same effect is found in the Fe group. In this case, the high-oxidation state of iron makes the tetrahedral low-spin situation the most favorable one, as discussed in the previous section, even if the high-spin state is rather close in energy. The move to its heavier congener, Ru^{IV} increases the relative stability of the low-spin form very

- (108) Figgis, B. N.; Hitchman, M. A. *Ligand Field Theory and its Applications*; Wiley-VCH: New York, 2000.
- (109) Griffith, J. S. *The Theory of Transition-Metal Ions*; Cambridge University Press: Cambridge, U.K., 1971.
- (110) Savage, P. D.; Wilkinson, G.; Motevalli, M.; Hursthouse, M. B. *Chem. Commun.* **1988**, 1349.
- (111) Arnold, J.; Wilkinson, G.; Hussain, B.; Hursthouse, M. B. *Chem. Commun.* **1988**, 1349.
- (112) Pillai, E. D.; Jaeger, T. D.; Duncan, M. A. *J. Am. Chem. Soc.* **2007**, *129*, 2297.
- (113) Tooze, R. P.; Stavropoulos, P.; Motevalli, M.; Hursthouse, M. B.; Wilkinson, G. *Chem. Commun.* **1985**, 1139.
- (114) Hay-Motherwell, R. S.; Wilkinson, G.; Hussain-Bates, B.; Hursthouse, M. B. *J. Chem. Soc., Dalton Trans.* **1992**, 3477.
- (115) Hay-Motherwell, R. S.; Wilkinson, G.; Hussain-Bates, B.; Hursthouse, M. B. *Polyhedron* **1991**, *10*, 1457.
- (116) García, M. P.; Jiménez, M. V.; Cuesta, A.; Siurana, C.; Oro, L. A.; Lahoz, F. J.; López, J. A.; Catalan, M. P.; Tiripicchio, A.; Lanfranchi, M. *Organometallics* **1997**, *16*, 1026.
- (117) García, M. P.; Jiménez, M. V.; Oro, L. A.; Lahoz, F. J.; Tiripicchio, M. C.; Tiripicchio, A. *Organometallics* **1993**, *12*, 4660.
- (118) Usón, R.; Forniés, J.; Tomás, M.; Menjón, B.; Sunkel, K.; Bau, R. *Chem. Commun.* **1984**, 751.
- (119) Fischer, D.; Hoppe, R.; Mogare, K. M.; Jansen, M. Z. *Naturforsch.* **2005**, *60b*, 1113.

Table 12. Experimental Geometry and Spin States for Homoleptic Complexes of Second and Third Transition Series Metals with σ -Donor Ligands and Electron Configurations d^3 – d^7

	metal	ligand	spin	geometry	φ_{T-SP} (%)	ref
d^3	Re ^{IV}	Tol	$1/2$	T	5	110
	Os ^V	Tol	$1/2$	T	11	111
d^4	Nb ^I	N ₂	2	SP	100	112
	Os ^{IV}	Cy	0	T	11	51
	Os ^{IV}	Tol	0	T	9	113
	Ru ^{IV}	Cy	0	T	10	51
	Ru ^{IV}	Tol	0	T	8	110
	Ru ^{IV}	Mes	0	T	15	114
	Os ^{IV}	Ph	0	T	3	51
	Ir ^V	Mes	0	T	19	114
d^5	Ir ^{IV}	Mes	$1/2$	T	NA ^a	115
d^7	Rh ^{II}	C ₆ Cl ₅	$1/2$	SP	100	116
	Ir ^{II}	C ₆ Cl ₅	$1/2$	SP	100	117
	Pt ^{III}	C ₆ F ₅	$1/2$	SP	99	118

^a The structure has been published, but the crystallographic data are not available.

much. It seems thus clear that the heavy transition metals should present a significantly different stereochemical behavior than the lighter element of the same group.

The stabilization of the tetrahedral low-spin stereoisomer for complexes with σ -donor ligands and heavy transition metals in low-oxidation states cannot be confronted at this point with experimental data because all the homoleptic complexes found (Table 12) correspond to metals in oxidation states +4 or +5, except for a couple of d^7 compounds, for which the square planar geometry is preferred in a low-spin configuration, just as predicted for [CoMe₄]²⁻ (Table 3). In contrast, the combined effect of a heavy transition metal and a high-oxidation state clearly favors the tetrahedral low-spin situation, as shown by all the examples of magnetically and structurally characterized homoleptic compounds with σ -donor ligands (Table 12).

If we focus on heavy transition metal compounds with π -donor ligands, we cannot just extrapolate the preference found for the high-spin state in the case of first transition series metals. Now there are two opposite effects. Thus, while π -donor ligands favor high-spin configurations, a heavier metal favors the low-spin one, especially for those electron configurations for which there is a small energy difference between low- and high-spin states in the presence of σ -donor ligands (i.e., d^7 and d^8 configurations, Figure 8). A systematic study of the potential energy surfaces for all d^n configurations of second and third row transition metals with π -donor ligands is out of the scope of this work. Nevertheless, we have carried out exploratory calculations for some specific examples. Thus the potential energy curves for [ReCl₄], [OsCl₄], and [IrCl₄] along the planarization pathway (Supporting Information) show that the low-spin state is stabilized and that the energy minimum of that spinomer is displaced from the tetrahedral shape to the sawhorse, as compared with the isoelectronic metals of the first transition series. The different stereoisomers, though, have similar energies.

The comparison of the theoretical predictions with experimental data is hampered by the scarcity of magnetic data found for this family of compounds. The available data for d^5 and d^6 complexes are in agreement with a preference of the heavy transition metal complexes with π -donor ligands

Table 13. Experimental Geometry and Spin States for Homoleptic Complexes of Second and Third Transition Series Metals with π -Donor Ligands

	metal	ligand	spin	geometry	φ_{T-SP} (%)	ref
d^2	Ru ^{VI}	O ²⁻	1	T	2	119
d^5	Ir ^{IV}	O ²⁻	$3/2$	SP	99	120
d^6	Pd ^{IV}	F ⁻	1	int.	59	121

for the intermediate spin configurations (Table 13). The d^5 SP4-[IrCl₄, $S = 3/2$] complex is noteworthy because it forms part of a group of isoelectronic compounds that appear as different stereoisomers, comprising T4-[CoCl₄, $S = 5/2$] and T4-[Co(Nor)₄, $S = 1/2$].

Magic Cube for Four-Coordinate Complexes

In the previous sections, we have seen that three main factors affect the relative energies of the different stereoisomers for a given electron configuration: the oxidation state of the metal atom, the transition series to which it belongs, and whether the ligands are π -donors. Some simple rules can be established on the basis of such an observation, regarding the preference of the tetrahedral stereoisomer for a high- or low-spin state, that apply to those electron configurations in which the spin dichotomy exists, that is, d^3 – d^6 . In so doing, we must not forget that in some cases an alternative stereoisomer with a different geometry may be energetically accessible, as seen in Figures 6–8. For that purpose, we have constructed the *magic cube* shown in Figure 12. We start by considering a compound of a light transition metal with π -donor ligands only and a low oxidation state (+3 or lower), represented by vertex **4** of the cube and expected to be more stable in its high-spin state. Going to a heavier transition metal, increasing the oxidation state, or replacing the ligands by π -donors can be represented

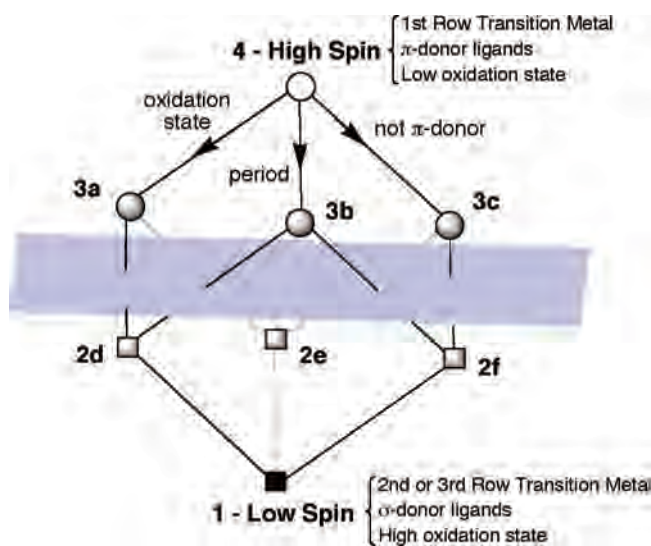


Figure 12. Magic cube for the prediction of the preferred spin state of tetrahedral complexes of transition metals with electron configurations between d^3 and d^6 . Starting from the uppermost vertex, which corresponds to a first transition series metal with π -donor ligands and an oxidation state of +3 or lower, a change in one of these parameters implies a displacement to a neighboring vertex as indicated by the arrows. Compounds whose characteristics correspond to vertices 3 and 4 are expected to be in a high-spin configuration, while compounds represented by vertices 1 and 2 are predicted to be low-spin ones.

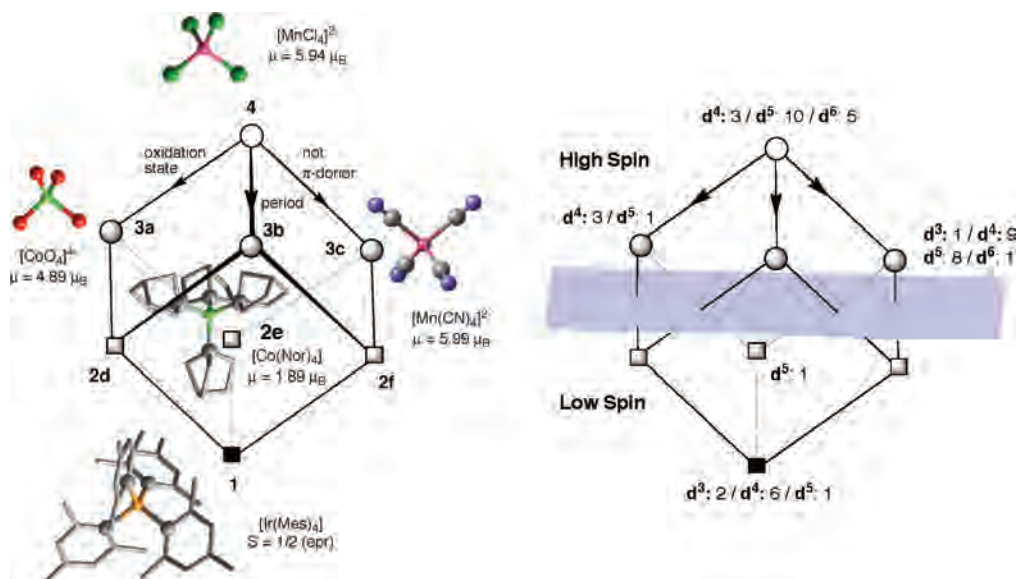


Figure 13. Examples of d^5 complexes that correspond to different vertices of the magic cube, together with their experimental magnetic moments (left) and summary of the homoleptic complexes identified for each vertex, according to the number of d electrons (right; more details provided as Supporting Information).

by displacements along three edges of the cube, leading to the three cases represented by gray circles (vertices **3a–c**), for which the low-spin state should be somewhat stabilized relative to the high-spin one, but probably not enough as to become the ground state. Changing two of those parameters at a time corresponds to a displacement through the diagonal of a cube's face, resulting in compounds represented by the gray squares (vertices **2d–f**), now more likely to be in a low-spin state. Finally, the modification of the three factors simultaneously should take us to the black square (vertex **1**), representing a case with clearly a low-spin ground state.

To show how the magic cube can help us understand the different geometries and spin states of apparently related compounds, let us consider a family in which several of its vertices have been experimentally identified (Figure 13), that of the d^5 complexes. Starting with $[\text{MnCl}_4]^{2-}$, with all the characteristics that favor a high-spin state and occupies vertex 4 of the magic cube, we can move to either vertex 3a or 3c by increasing the oxidation state or replacing the π -donor ligands by cyanides, respectively, while still retaining the high-spin configuration in $[\text{CoO}_4]^{4-}$ and $[\text{Mn}(\text{CN})_4]^{2-}$. The simultaneous change of those two parameters is represented by the high-oxidation state complex with σ -donor ligands $[\text{Co}(\text{Norbornyl})_4]$, corresponding to vertex 2e, whose magnetic moment is in agreement with the qualitative prediction of the magic cube. A further change of cobalt by the heaviest element of the group in $[\text{Ir}(\text{Mes})_4]$ takes us to the lowest vertex 1, also representative of a low-spin configuration.

Among the homoleptic complexes with d^3 – d^6 configurations and tetrahedral geometry (Tables 5, 6, 9, 12, and 13, collected as an independent table in Supporting Information), we have found no exception to the expectations of the magic cube regarding the high-or low-spin ground state. It must be mentioned, however, that we have identified only one representative of vertex 2e and only one computational example of vertex 2d, corresponding to $[\text{PdF}_4]$,¹²¹ whereas

we are not aware of the existence of any tetrahedral complex with the characteristics of vertices 2f or 3b. These are, therefore, highly interesting synthetic targets. The number of magnetically and structurally characterized complexes that correspond to the different situations represented by the magic cube with each d^n configuration is shown in Figure 13 (right).

The discussion of the stereospinomeric preferences of four-coordinate complexes carried out up to this point has focused essentially on homoleptic complexes. A more detailed analysis of how the general rules established here can be modified in the presence of mixed ligands is outside the scope of the present work. Nevertheless, we have reported a preliminary study²⁰ of two such cases that suggest how a set of ligands with different donor properties may modify the d block orbital splitting pattern, thus modifying the stereospinomeric preferences. This is what happens with $[\text{NiBr}(\text{norbornyl})_3]$, a tetrahedral diamagnetic Ni^{IV} complex with one π -donor and three σ -donor ligands reported by Dimitrov and Linden.¹²² Let us recall that for homoleptic complexes with either σ -donor or π -donor ligands, we expect two stereospinomers to have similar energies, a tetrahedral quintet and a square planar triplet (Figure 8 and Supporting Information), whereas the singlet state is predicted to be at much higher energy in both cases. But the introduction of just one π -donor ligand makes this compound diamagnetic. Calculations on this specific compound in its experimental tetrahedral geometry and on its theoretical analog $[\text{NiBrMe}_3]$ correctly predict the low-spin configuration to be the most stable one. This situation was explained by a d orbital splitting pattern analogous to that of the octahedron (two over three) because of the presence of a significant umbrella-type distortion combined with the strong π -interaction of the bromide with only two of the five d orbitals.²⁰

(121) Aullón, G.; Alvarez, S. *Inorg. Chem.* **2007**, *46*, 2700.

(122) Dimitrov, V.; Linden, A. *Angew. Chem., Int. Ed.* **2003**, *42*, 2631.

Concluding Remarks

A qualitative molecular orbital analysis of the d-block orbitals in four-coordinate transition metal complexes with σ -donor ligands allows us to classify the various spin states of all d^n electron configurations in three families according to their d orbital occupation and expected stereochemistry. Starting from the most symmetric structure, the tetrahedron, nontetrahedral structures are predicted as a result of Jahn–Teller distortions. The lowest two metal d orbitals (the e set of the tetrahedron) are stereochemically inactive, and consequently, all electron configurations in which the three t_2 orbitals have the same occupation are expected to be tetrahedral, regardless of the occupation of the e set. When one of the t_2 orbitals has a lesser occupation than the other two, a nearly square planar geometry is to be expected, whereas lower-symmetry structures with an approximate sawhorse shape should appear when one t_2 orbital has a higher occupation than the other two. Those stereochemical rules are supported by DFT geometry optimization of 21 spin states of first transition series $[\text{MMe}_4]^{n-}$ complexes with all d^n electron configurations.

First transition series metals with σ donor ligands and a number of d electrons that give rise to only one spin state (d^0 , d^1 , d^2 , d^9 , and d^{10}) are all predicted to present tetrahedral coordination spheres with the exception of the d^9 case. For that configuration, given the flat potential energy surface, important structural variability is to be expected. Among metals in low-oxidation states (+3 or lower) and electron configurations that allow for two or three spin states, the d^4 – d^7 ions are predicted to be more stable as high-spin tetrahedral stereospinomers, whereas for the d^3 and d^8 cases the low-spin stereospinomers (tetrahedral and square planar, respectively) are also competitive. The stereospinomeric preferences can be modified by a higher oxidation state of the metal atom or by the π -donor nature of the ligands. Hence, π -donor ligands stabilize the high-spin configurations, whereas a high-oxidation state (+4) stabilizes the low-spin one for d^3 – d^6 ions.

Although we have analyzed in this work only compounds with monodentate ligands, we should keep in mind that bi- or multidentate ligands can influence the geometrical choice, as discussed in a previous work.² For instance, it was found that bidentate ligands with small normalized bites, such as dithiocarbamates, tend to appear only in square planar geometry (except for complexes of the post-transition Zn^{II} and Hg^{II} ions), whereas ligands with larger bites, such as ethylenediamine, bipyridine, or dithiolates can adapt to both tetrahedral and square-planar coordination spheres and should thus be expected to follow the same rules deduced here for monodentate ligands. Since each spin state has a distinct stereochemical preference, the choice of rigid multidentate ligands can stabilize spin states that are unstable in the presence of monodentate ligands. This is what happens with porphyrinato, phthalocyaninato, and related tetradentate

macrocyclic ligands that appear in intermediate spin states, such as $S = 3/2$ for d^5 or $S = 1$ for d^6 ions.

Since we have seen that it is quite common to find structures intermediate between tetrahedral and square planar, we propose to complement the stereochemical descriptor when needed, by addition of the value of the generalized coordinate along the polyhedral interconversion path. For instance, the most stable stereospinomer for the d^4 Mn^{III} ion that is approximately square planar but with a significant distortion toward the tetrahedron, could be formulated as $SP4(27\% T4)$ - $[\text{MnMe}_4, S = 2]^-$ to indicate that it falls approximately along the interconversion pathway between those two shapes (as evidenced by a relatively small value of the path deviation function, not given) and that the distortion reaches a 27% along the way toward the tetrahedron.

The factors that favor the choice of a low-spin state for a tetrahedral compound are the absence of π -donor ligands, a high-metal oxidation state (+4 or higher), and the pertence of the metal to the second or third transition series. Combinations of these factors result in eight different situations that can be accommodated in a magic cube that seems to have interesting predictive abilities. The types of compounds for which we have been unable to identify structurally characterized examples constitute interesting synthetic targets. These correspond to vertices 2d (a heavy metal in a high-oxidation state with π -donor ligands) and 2f (heavy metal in a low-oxidation state with σ -donor or π -acceptor ligands) of the magic cube, both predicted to prefer a low-spin configuration. Similarly, we have found no example of compounds of type 3b (heavy metal in a low-oxidation state with π -donor ligands), expected to prefer a high-spin state. Also worth pursuing are the low-spin complexes of type 2e (first row transition metal in a high-oxidation state with σ -donor or π -acceptor ligands), as well as complexes of second or third transition series metals with π -donor ligands in a high-oxidation state (type 2d), two cases for which we have found only one representative.

Notwithstanding the many factors that participate in the determination of stereochemistry and spin state of four coordinate complexes, a broad description of the main structural trends for a d^n electron configuration is obtained by comparing a histogram of the structural frequency at given intervals of the generalized coordinate with the potential energy curves calculated for the different spin states of the first transition series methyl complexes (Figures 4–8). As shown previously for the d^6 case,²⁰ nearly isoenergetic energy minima are reflected in maxima of the experimental distribution of structures. We further illustrate such a behavior here with the case of the d^7 compounds (Figure 14) that present a maximum in the number of structures centered close to the tetrahedron ($\varphi_{\text{T-SP}} \approx 0$) in correspondence with the minimum in energy for the high-spin state. The second maximum of structures, centered at the square ($\varphi_{\text{T-SP}} \approx 100\%$), corresponds to the energy minimum for the low-spin state. Such a correspondence between the two plots suggests that the two groups of structures should correspond to the tetrahedral high-spin and square planar low-spin

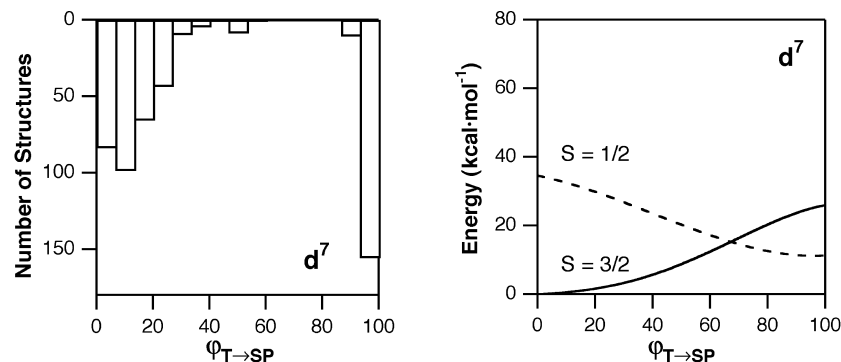


Figure 14. Comparison of the maxima in the distribution of experimental structures of d^7 complexes along the tetrahedron-square pathway with the minima in the calculated energy for the two spin states of $[\text{CoMe}_4]^{2-}$.

stereospinomers, respectively. All the square planar complexes in that plot for which the spin state has been characterized are indeed in the low-spin configuration (references and magnetic moments given as Supporting Information).

Similar histograms are provided for all other d^n configurations as Supporting Information. In general, the distribution of the experimental structures mirrors the well of the potential energy surface, thus providing a nice illustration of the structural correlation principle.¹²³ Apparent inconsistencies can find an explanation by closer inspection. Such is the case of the d^9 ions, for which the square planar structure is expected to be less common than intermediate geometries, according with the shape of the potential energy curve of the methyl complex (Figure 5). The fact that it is precisely the square planar geometry that appears as the most common one can be explained because most of those correspond in fact to Jahn–Teller distorted six-coordinate complexes, with “non-bonded” metal–ligand distances covering all the range between 2.4 and 3.2 Å. Other exceptions have already been discussed above and result from the constrained square planar geometry imposed by some macrocyclic ligands (e.g., in Zn^{II} complexes) or the nearly tetrahedral coordination imposed by tri- or tetradentate tripod ligands.

Computational Details

DFT calculations were carried out with the Gaussian03 code¹²⁴ using the B3LYP hybrid functional¹²⁵ and the quadratic convergence approach, with a guess function generated with the Jaguar program.¹²⁶ The triple- ζ all-electron Gaussian basis set proposed by Schaefer et al. was employed,¹²⁷ together with the SDD pseudopotentials¹²⁸ for metals of the second transition series.

The reliability of the DFT calculations for the evaluation of relative energies of different spin states was tested with the $[\text{MMe}_4]^{2-}$ homoleptic complexes ($M = \text{Cr}, \text{Mn}$), for which both structural and magnetic experimental data are available.^{58,129} As a test of the performance of the DFT methodology applied, we compare here some experimentally observed electronic transition energies with the values obtained through TD-DFT calculations¹³⁰ (Table 14), for which a fair agreement was found. Furthermore, the energy gap between the e and t_2 orbitals is also in semiquantitative

Table 14. Calculated and Experimental¹⁰⁷ Energies (cm^{-1}) for the Lowest Spin-Allowed Electronic Transition of $[\text{MCl}_4]^{2-}$ Anions, Together with Their Kohn–Sham Orbital Gap (Δ_i)

metal	spin	Δ_i (DFT)	$\nu(\text{TD-DFT})$	$\nu(\text{exptl})$
Cr^{II}	2	8450	8340	9800
Fe^{II}	2	3930	3520	4050
Ni^{II}	$3/2$	2380	4860	6550
Cu^{II}	$1/2$	18 800	17 500	17 000

agreement with the energies of the first electronic transition observed for some $[\text{MCl}_4]^{2-}$ anions

Experimental structural data for homoleptic complexes reported in this paper were retrieved from the Cambridge Structural Database (CSD, version 5.28) through searches of four-coordinate transition-metals in mononuclear complexes with single bonds to C-donor atoms (σ -donor ligands), halogens, or chalcogens (π -donor ligands), excluding direct bonds between donor atoms. These searches were restricted to nonpolymeric structures with no disorder and R factors of at most 10%. Further structural information was obtained from the Karlsruhe Inorganic Crystal Structures Database. The structural data used for the histograms presented in Figure 14 and as Supporting Information were obtained mostly from the CSD (version 5.23),³⁵ using search criteria described elsewhere.² Shape measures, deviation functions, and generalized coordinates were calculated with the SHAPE program.¹³¹

Acknowledgment. Support from the Dirección General de Investigación (MEC), project CTQ2005-08123-C02-

(123) (a) Bürgi, H.-B. In *Perspectives in Coordination Chemistry*; Williams, A. F., Floriani, C., Meerbach, A. E., Eds.; Verlag Helvetica Chimica Acta: Basel, Switzerland, 1992; (b) Bürgi, H.-B.; Dunitz, J. D., Eds. *Structure Correlations*; VCH: Weinheim, Germany, 1994.

(124) Frisch, M. J.; Trucks, G. W.; Schlegel, H. B.; Scuseria, G. E.; Robb, M. A.; Cheeseman, J. R.; Montgomery, J. A., Jr.; Vreven, T.; Kudin, K. N.; Burant, J. C.; Millam, J. M.; Iyengar, S. S.; Tomasi, J.; Barone, V.; Mennucci, B.; Cossi, M.; Scalmani, G.; Rega, N.; Petersson, G. A.; Nakatsuji, H.; Hada, M.; Ehara, M.; Toyota, K.; Fukuda, R.; Hasegawa, J.; Ishida, M.; Nakajima, T.; Honda, Y.; Kitao, O.; Nakai, H.; Klene, M.; Li, X.; Knox, J. E.; Hratchian, H. P.; Cross, J. B.; Bakken, V.; Adamo, C.; Jaramillo, J.; Gomperts, R.; Stratmann, R. E.; Yazyev, O.; Austin, A. J.; Cammi, R.; Pomelli, C.; Ochterski, J. W.; Ayala, P. Y.; Morokuma, K.; Voth, G. A.; Salvador, P.; Dannenberg, J. J.; Zakrzewski, V. G.; Dapprich, S.; Daniels, A. D.; Strain, M. C.; Farkas, O.; Malick, D. K.; Rabuck, A. D.; Raghavachari, K.; Foresman, J. B.; Ortiz, J. V.; Cui, Q.; Baboul, A. G.; Clifford, S.; Cioslowski, J.; Stefanov, B. B.; Liu, G.; Liashenko, A.; Piskorz, P.; Komaromi, I.; Martin, R. L.; Fox, D. J.; Keith, T.; Al-Laham, M. A.; Peng, C. Y.; Nanayakkara, A.; Challacombe, M.; Gill, P. M. W.; Johnson, B.; Chen, W.; Wong, M. W.; Gonzalez, C.; Pople, J. A. *Gaussian 03*, revisions C.1 and C.4; Gaussian, Inc.: Pittsburgh, PA, 2003.

(125) Becke, A. D. *J. Chem. Phys.* **1993**, *98*, 5648.

(126) *Jaguar 6.0*, release 11; Schrödinger, LLC: New York, 2005.

(127) Schaefer, A.; Huber, C.; Ahlrichs, R. *J. Chem. Phys.* **1994**, *100*, 5829.

(128) Andrae, D.; Haeussermann, U.; Dolg, M.; Stoll, H.; Preuss, H. *Theor. Chim. Acta* **1990**, *77*, 123.

(129) Morris, R. J.; Girolami, G. S. *J. Am. Chem. Soc.* **1988**, *110*, 6245.

(130) Casida, M. E.; Jamorski, C.; Casida, K. C.; Salahub, D. R. *J. Chem. Phys.* **1998**, *108*, 4439.

02BQU, and from Comissió Interdepartamental de Ciència i Tecnologia (CIRIT), grant 2005SGR-00036, is acknowledged. J.C. thanks MEC for an FPU grant (reference AP2002-2236). The authors are grateful to B. Menjón and J. Forniés for providing them with structural data prior to its publication, and to D. Avnir and D. Casanova for discussions. The authors thank the CESCA Supercomputing Center for the allocation of computer time.

Supporting Information Available: Atomic coordinates for the optimized stereoisomers of four-coordinate complexes with methyl or chloro ligands; structural and magnetic data for porphyrinato and related complexes; cross sections of the

(131) Llunell, M.; Casanova, D.; Cirera, J.; Bofill, J. M.; Alemany, P.; Alvarez, S.; Pinsky, M.; Avnir, D. *SHAPE*, version 1.1; Universitat de Barcelona and The Hebrew University of Jerusalem: Barcelona, Spain, 2003.

potential energy surfaces along the tetrahedron to square planar interconversion path for methyl and chloro complexes; experimental magnetostructural data for complexes with π -donor ligands of d^0 , d^1 , d^2 , d^5 , d^6 , d^7 , and d^{10} electron configurations; atomic coordinates and structural information for the optimized stereoisomers of methyl complexes of the first transition series in a high (+4) oxidation state; atomic coordinates of the optimized structures of Mo^{II} , Ru^{IV} , and Ir^{IV} methyl complexes; geometries and spin states of tetrahedral homoleptic compounds with d^3 – d^7 electron configurations and their relationship with the magic cube; histograms showing the distribution of geometries of all four-coordinate complexes in the CSD along the tetrahedron to square planar pathway with a given d^n electron configuration; and CSD refcodes and magnetic moments (or spin state) of square planar four-coordinate compounds of d^4 and d^7 ions.

IC702276K